Adv in Biophys (2003) Vol.37, pp. 1-48

Brain neurosteroids are 4th generation neuromessengers in the brain: Cell biophysical analysis of steroid signal transduction

Department of Biophysics and Life Sciences, Graduate School of Arts and Sciences, University of Tokyo at Komaba, Meguro, Tokyo 153, Japan

Suguru Kawato[a], Makoto Yamada[b] and Tetsuya Kimoto

General Introduction

This work reviews recent achievements made by our lab. on intercellular signal transduction related to the synthesis and action of steroids. These achievements were made possible by the high suitability of cytochrome P450, a key enzyme in signal transduction, to quantitative spectroscopic analysis. Both digital microscopic imaging, electrophysiology analysis and time–resolved protein rotation measurements were used: Real–time microscopic imaging was used to investigate Ca^{2+} signaling, endosome trafficking and P450scc activity; Electrophysiology was necessary to examine synaptic neuron–neuron communication; Protein rotation was used to analyze molecular mechanisms of electron transfer in cytochrome P450 systems.

Steroid hormones, including sex hormones, play an essential role in the homeostasis of the body, allowing the mediation of genomic processes via nuclear steroid hormone receptors. In a classical view, steroid hormones are modeled as being synthesized exclusively in peripheral organs such as the adrenal cortex and the gonads. They then reach the target tissues via blood circulation. Recently, however, steroids have been shown to be present in the brain. These brain neurosteroids have been demonstrated to act acutely (<30min) on neurotransmitter receptors located on the cell membranes in the hippocampus (the center for learning and memory), the amygdala (the center for emotional behavior), the retina and the olfactory bulb, and, as such, are likely to play an essential role in signal transduction processes related to learning, memory and emotional response. One example, the postsynaptic neuron activation circuit, consisting of neurosteroidogenic systems and the N-methyl-D-aspartate (NMDA) receptors of the hippocampus, was discovered in this laboratory.

Although the physiological roles of these brain neurosteroids have not been sufficiently elucidated, it is

[a]To whom correspondence should be addressed.

FAX/TEL: 81-3-5454-6517, E-mail : kawato@phys.c.u-tokyo.ac.jp

[b]Present address: Kyorin University School of Medicine, Mitaka, Tokyo 181, Japan

Abbreviations

ADR, NADPH-adrenodoxin reductase; ADX, adrenodoxin; CORT, corticosterone

Cytochrome P450scc, cytochrome P450 having cholesterol side-chain cleavage activity ; Cytochrome P45017α, cytochrome P450 catalyzing the 17α–hydroxylation of pregnenolone; Cytochrome P450c21, cytochrome P450 catalyzing 21–hydroxylation of progesterone; Cytochrome P450arom, cytochrome P450 catalyzing aromatization of androstendione; Cytochrome P45011β, cytochrome P450 catalyzing 11β–hydroxylation of deoxycorticosterone and deoxycortisol; DHEA, dehydroepiandrosterone; GABA, γ–aminobutyric acid ; GFAP, glial fibrillary acidic protein ; 3β-HSD, 3β–hydroxysteroid dehydrogenase; 17β–HSD, 17β–hydroxysteroid dehydrogenase; MBP, myelin basic protein ; NMDA, N–methyl–D–aspartate; PREG, pregnenolone; PREGS, pregnenolone sulfate; RIA, radioimmunoassay; StAR, steroidogenic acute regulatory protein

possible that their actions may be completely different from those of peripheral steroids. Here we propose that brain neurosteroids are 4th generation neuromessengers which are synthesized within the neurons and are responsible for acute modulation of neuron–neuron communication through neurotransmitter receptors. First generation neuromessengers are neurotransmitters such as glutamate, GABA and acetylcholine; Second generation neuromessengers are catecholamines such as dopamine and serotonin; Third generation neuromessengers are neuropeptides such as Enkephalin, vasoactive intestinal peptide, and substance P. Although 1st–3rd generation neuromessengers are stored in synaptic vesicles, and are rapidly exocytosed from presynapses, neurosteroids are produced in mitochondria and microsomes driven by Ca^{2+} signals, and released by passive diffusion as paracrine messengers. The techniques of cell biophysics, in combination with biochemistry and molecular biology, could be a powerful method of investigating molecular mechanisms of the action and synthesis of brain steroids, an exciting new field for the 21st century.

Chap. 1 Neurosteroids: a novel family of neuroactive messengers essentially contributing to long–term potentiation, learning and memory

Introduction

Brain neurosteroids are neuroactive steroids which are synthesized *de novo* in the brain (1). Recent studies revealed the presence of significant amounts of neurosteroids such as pregnenolone (PREG), dehydroepiandrosterone (DHEA) and their sulfate esters (PREGS and DHEAS) in the mammalian brain (2). Adrenalectomy did not decrease the level of PREG(S) and DHEA(S) in the brain (3). Neurosteroidogenesis has, however, not been well elucidated, due to the extremely low levels of steroidogenic proteins in the brain. In contrast to the classical genomic effects of peripheral steroids, many neurosteroids induce acute physiological actions on cell surface receptors (4 – 6).

There is increasing evidence that neurosteroids modulate neurotransmissions acutely (<30min), with either excitatory or inhibitory effects, in the hippocampus (1). PREGS potentiated the Ca^{2+} conductivity of the NMDA subtype of glutamate receptors (7, 8) but suppressed the Cl^- conductivity of the γ–aminobutyric acid (GABA) receptors in cultured rat hippocampal neurons (9, 10). In combination, these actions could facilitate excitation of neurons at the postsynaptic level (9). DHEA potentiates the GABA–induced Cl^- current but DHEA sulfate (DHEAS) suppresses it (9–11). 17β–estradiol is an estrogen which may be synthesized by P450arom in the hippocampus as well as the gonads. A few reports present the possible acute effect of estradiol on neuronal excitability in the hippocampus (12–14).

Neurosteroids are indicated to be effective in learning and memory of animals. The administration of PREGS and DHEA enhanced the retention of footshock avoidance in mice when injected directly into the hippocampus (15, 16). An injection of PREGS into the hippocampus temporally improves the spatial memory performance of deficient aged rats (1, 17).

The location and activity of the neurosteroidogenic machinery in the brain has not been sufficiently elucidated. Many studies showed mainly that the mRNAs of steroidogenic enzymes were expressed at low levels in the entire cerebrum and cerebellum. For example, the amount of P450scc mRNA expressed in the brain was extremely small, around $1/10^4$ –$1/10^5$ of that in the adrenal gland (18, 19).

Neurosteroid synthesis in the brain might be catalyzed by biotransformation of cholesterol to various steroids by the cytochrome P450–containing monooxygenase systems as hypothetically illustrated in Figures 1 and 2. Cholesterol is transported into the mitochondria with steroidogenic acute regulating protein (StAR). In the mitochondria, cytochrome P450scc (CYP11A1) catalyzes the side–chain cleavage of cholesterol, resulting in pregnenolone formation, which is promoted by electron transfer from NADPH to P450scc through NADPH–adrenodoxin reductase (ADR) and adrenodoxin (ADX). PREG reaches the microsomes (endoplasmic reticulum), where cytochrome P45017α„lyase (CYP17) catalyzes the 17α‚–hydroxylation of pregnenolone, resulting in the formation of DHEA. After the transformation of DHEA to androstenedione by 3β-hydroxysteroid dehydrogenase (3β-HSD), cytochrome P450aromatase (P450arom, CYP19) catalyzes the conversion of androstenedione to estrone. This is followed by a further transformation to 17β–estradiol by 17β–hydroxysteroid dehydrogenase (17β–HSD). Testosterone is also formed from androstenedione by 17β–HSD. The possible conversion of testosterone to17β–estradiol may be performed by P450arom.

Hydroxysteroid sulfotransferase converts PREG and DHEA to their sulfate forms, PREGS and DHEAS. In another pathway in microsomes, PREG is metabolized to progesterone by 3β-HSD. Cytochrome P450c21 converts progesterone to deoxycorticosterone and deoxycortisol, which then reach the mitochondria, where P45011β converts them to corticosterone (CORT) and cortisol, respectively. Cytochromes P45017α, P450c21 and P450arom accept electrons from NADPH–cytochrome P450 reductase. It should be noted that little was known about the existence and localization of P450scc, P45017α,, P450arom and sulfotransferase in brain neurons such as hippocampal neurons prior to our studies. The presence of mRNAs for 17β-HSD (20, 21) and P450c21 (22) was indicated in the brain.

1. 1 Localization of functional neurosteroidogenic systems in pyramidal neurons in the rat brain hippocampus

In the hippocampus, there was no direct demonstration of the localization of steroidogenic machinery. We have presented the first demonstration of the presence and activity of complete steroidogenic systems in the hippocampal neurons from adult male rats (23, 24).

Immunohistochemical and Western immunoblot analysis

A significant localization for cytochromes P450scc, P45017α, and P450arom was successfully observed in pyramidal neurons in the CA1–CA3 regions, as well as granule cells in the dentate gyrus, with immunohistochemical staining of slices. Co–localization of P450s with redox partners, hydroxysteroid sulfotransferase and StAR was also demonstrated in pyramidal neurons and granule cells.

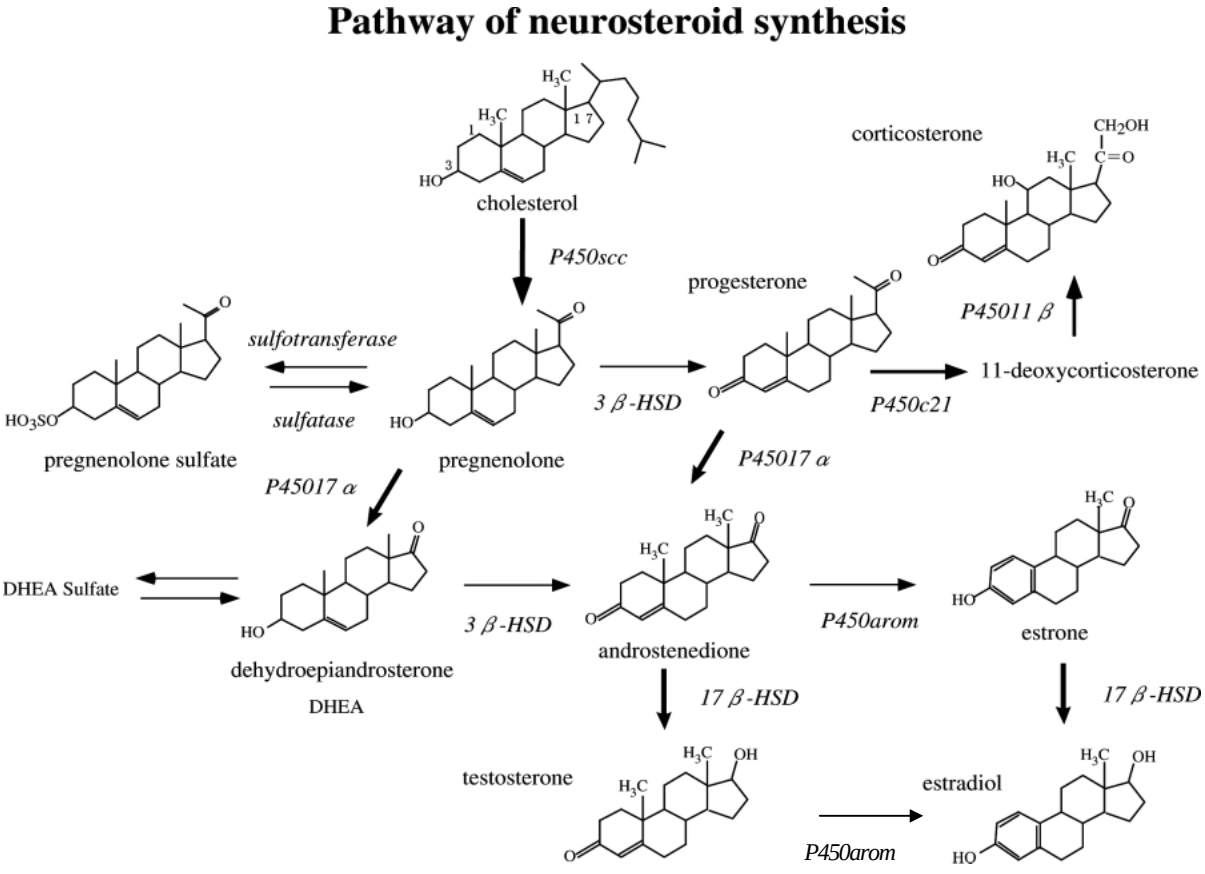

Figure 1

Flow chart of brain neurosteroid synthesis in the hippocampal neurons. The structures of neurosteroids and enzymes responsible for biotransformation. P450scc and P45011β are in the mitochondria. P45017α, P450c21 and P450arom are in microsomes. P450c21 is lacking in the gonadals, and P450arom and 17β–HSD are lacking in the adrenal glands.

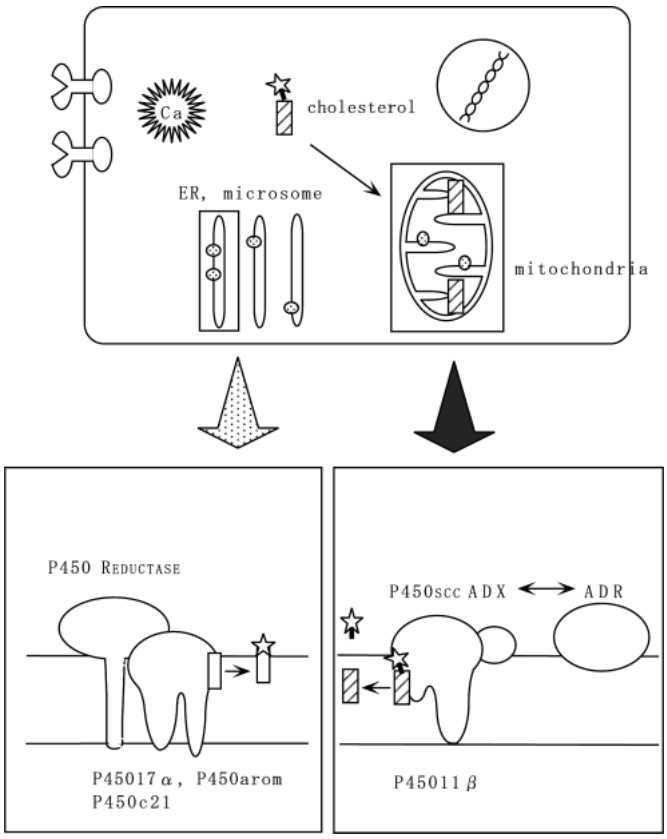

Figure 2

Schematic model illustration for the topological arrangement of cytochrome P450 systems in mitochondria and microsomes (endoplasmic reticulum, E R). Upon electron transfer from reductases to P450s, P450s activate oxygen, resulting in steroid hydroxylation.

To determine the localization of P450scc, an immunohistochemical staining was performed with anti–rat P450scc antibodies raised against a peptide sequence (amino acids 421–441) using the avidin–biotin–peroxidase complex (ABC) technique according to the free–floating method (25) (Fig. 3). An intense immunoreaction with P450scc IgG was restricted to pyramidal neurons in the CA1–CA3 regions as well as granule cells in the dentate gyrus. The co–localization of immunoreactivity against P450scc and neurofilaments showed that P450scc was present in the neurons. Preadsorption of the antibody with excess purified bovine P450scc antigen resulted in complete absence of P450scc immunoreactivity in all of the positively stained cells in the hippocampus (Fig. 3), due to the crossreaction of the anti-rat

P450scc antibodies which we used (24). Essentially the same P450scc staining pattern was observed in male and female rats.

Immunohistochemical staining was also performed for other cytochrome P450s such as P45017α, and P450arom, using anti–guinea pig P45017α, IgG (gift from Dr. Shiro Kominami) and anti–human P450arom IgG (gift from Dr. Nobuhiro Harada**)** (Fig.4). The sulfotransferase and StAR were also stained with antibodies against rat hydroxysteroid sulfotransferase (gift from Dr. Hiro-omi Tamura) and mouse StAR (gift from Dr. Douglas Stocco). 3β–HSD activity was obtained with formazan accumulation. The presence of redox partners of P450scc was examined using immunostaining with antibodies against beef ADR and ADX (gift from Dr. Takayuki Hara) (Fig. 5). Intense immunoreaction with all these antibodies was restricted to pyramidal neurons in the CA1–CA3 regions and granule cells in the dentate gyrus.

The 3β–HSD activity was also localized in these neurons. These results imply that pyramidal neurons and granule cells have complete steroidogenic systems which catalyze (1) the conversion of cholesterol to PREG driven by electron transport from NADPH to P450scc through ADR and ADX, (2) further conversion to progesterone and DHEA, (3) sulfation to PREGS and DHEAS, and (4) possible conversion to testosterone and estradiol (see Fig. 1).

The expression of proteins was confirmed by Western immunoblot analysis for P450s, redox partners, hydroxysteroid sulfotransferase and StAR from the hippocampus. As illustrated in Fig. 6, a single protein band was observed for each of these proteins. The molecular weight of the P450scc band in isolated mitochondria was almost identical to that of bovine adrenocortical P450scc (approximately 54 kDa). The molecular weights of P45017α, and P450arom in microsomes, ADR and ADX in

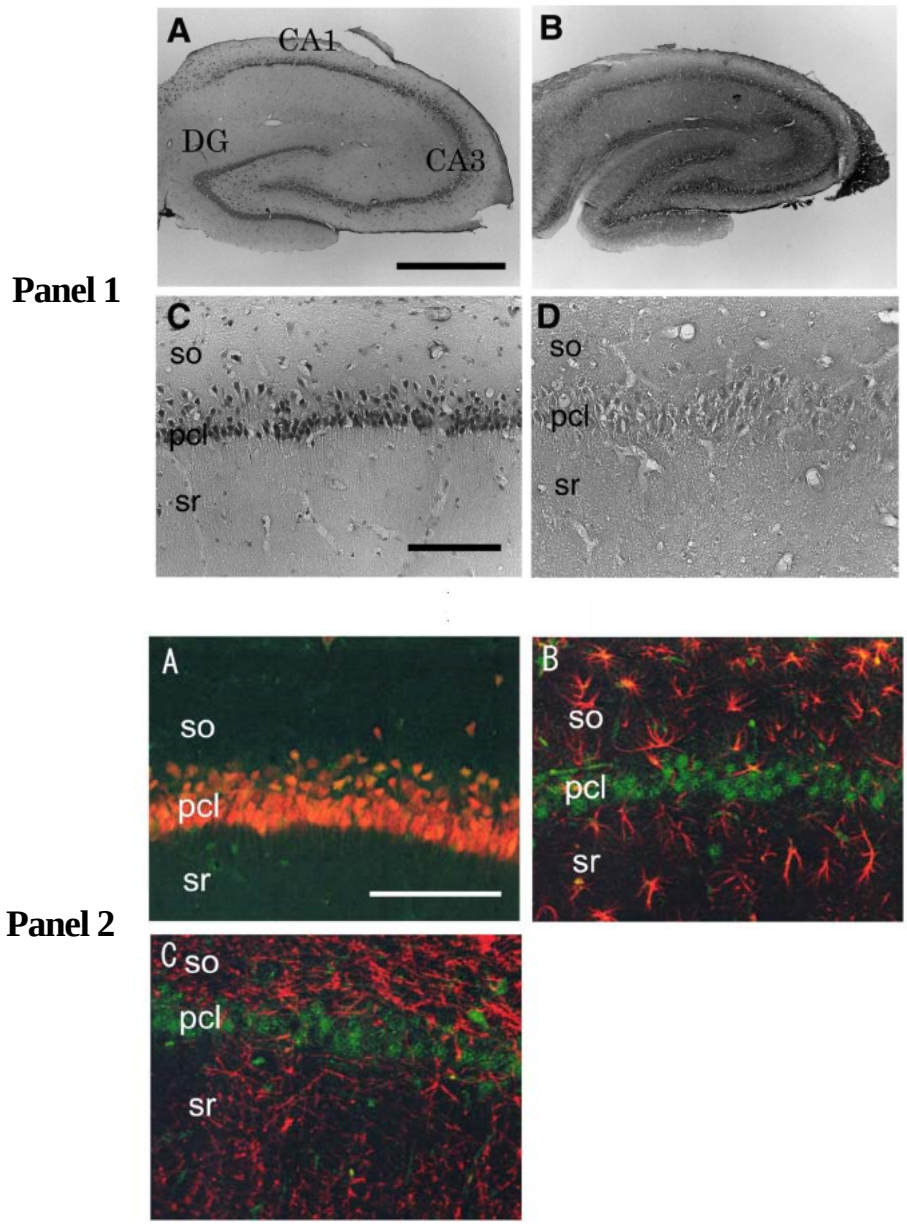

Figure 3

Immunohistochemistry of cytochrome P450scc in hippocampal slices of an adult male rat. The somata layer of pyramidal neurons is characterized as a mirror image of C–shaped curve throughout the CA1– CA3 regions of the hippocampus. Granule cells in the dentate gyrus (DG) showed a characteristic arrowhead distribution. Panel 1 : **A**, Low magnification image of the whole hippocampus stained with antibodies against rat cytochrome P450scc; **B**, Neurofilaments stained with anti–neurofilament 200 IgG; **C**, The hippocampal CA1 region stained with antibodies against rat P450scc; **D**, Staining with anti–P450scc IgG preincubated with a saturating concentration of purified P450scc in the CA1 region. Note that A and B are at low magnification; C and D are at identical high magnification. *Scale bar*, 800 μm (**A** and **B)**, and 120 μm (**C** and **D)**. Immunoreactive cells were visualized using diaminobenzidine–nickel staining. Panel 2 : **A**, confocal fluorescence dual staining of P450scc (green) and neuronal nuclear antigen (red); **B**, fluorescence dual staining of P450scc (green) and GFAP (red); **C**, fluorescence dual staining of P450scc (green) and MBP (red). A superimposed region of green and red fluorescence is represented in yellow. **A**–**C**, the same high magnification. *Scale bar* ,120 μm (**A**–**C)**. so, stratum oriens; pcl, pyramidal cell layer; sr, stratum radiatum.

mitochondria were approximately 57, 57, 54 and 12 kDa, respectively. The molecular weight of the sulfotransferase, 30 kDa, in cytoplasmic fractions was slightly smaller than that of the purified rat liver protein. Only the full–length 37 kDa

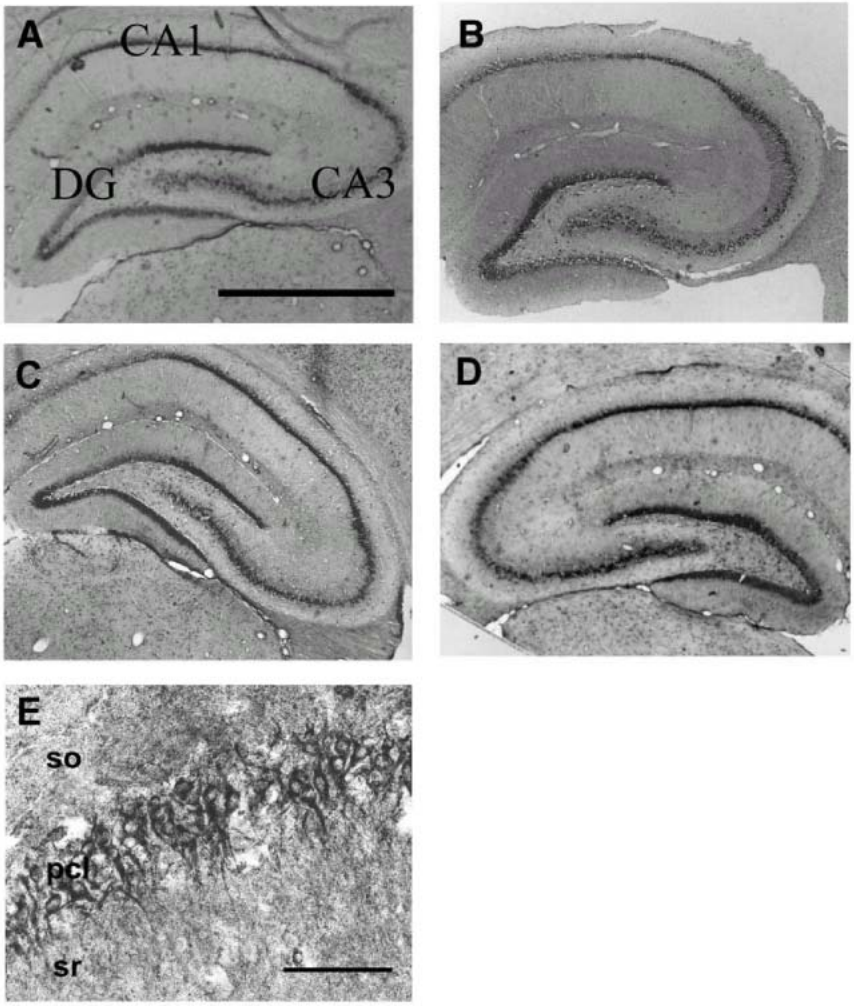

Figure 4

Immunohistochemical staining with antibodies against P45017α,, P450arom, the sulfotransferase and StAR in the hippocampus of an adult male rat. **A**, P45017α, in the whole transverse section of the hippocampus; **B**, P450arom; **C**, the sulfotransferase; **D**, StAR protein; **E**, Activity of 3β–HSD in the CA1 region revealed by nitro–BT staining. P45017α,, P450arom, the sulfotransferase, StAR and 3β–HSD are restricted to pyramidal neurons in the CA1–CA3 regions and granule cells in the dentate gyrus (DG). **A, B, C, D** a low magnification; **E**, the high magnification. *Scale bar*, 800 μm (**A – D)** and 120 μm (**E)**. Immunoreactive cells in **A**–**D** are visualized with diaminobenzidine–nickel staining.

species of StAR in the mitochondria was observed in the control hippocampus. When the hippocampus was stimulated by 100 μM NMDA for 30 min, the conversion of StAR from the 37 kDa species to the truncated 30 kDa species was observed (see Fig. 6, Panel B). The processing of StAR proteins was dependent on an NMDA–mediated–Ca^{2+} influx. This processing of StAR may coincide with the Ca^{2+} –dependent movement of StAR bearing cholesterol from the outer to the inner membranes of mitochondria, supplying cholesterol to P450scc.

The role of neurons on neurosteroid synthesis in the hippocampus had not been clearly described prior to our study. The distributions of some steroidogenic proteins in the hippocampus were recently demonstrated by means of in situ hybridization. The distribution of StAR mRNA and 3β–HSD mRNA ($1/10^2$ –$1/10^3$ of the levels in the adrenal gland) was localized along the pyramidal cell layer in the CA1–CA3 regions and the granule cell layer in the dentate gyrus, while the amount of P450scc mRNA in these neurons was shown to be extremely low (26, 27).

For decades, many investigators have believed neurosteroidogenesis to be carried out mainly in glial cells, because anti–bovine P450scc antibodies are absorbed by the white matter throughout the rat brain (28, 29), and because many reports have indicated the presence of P450scc, although at low levels, in astrocytes, oligodendrocytes and white matter (28, 30, 31). We therefore examined the possible existence of P450scc in glial cells. The distributions of astroglial cells and oligodendroglial cells showed, however, very different patterns from that of the P450scc–containing cells **(**see Fig.3**)**. Antibodies against glial fibrillary acidic protein (GFAP), a marker protein of astroglial cells, stained astro–shaped cells in the stratum radiatum and the stratum oriens in the hippocampus. The antibodies against myelin basic protein (MBP), a marker protein of oligodendroglial cells, stained many long fibril cells. The distributions and shapes of GFAP–reactive cells and MBP–reactive cells are very different from those of P450scc–reactive cells, indicating

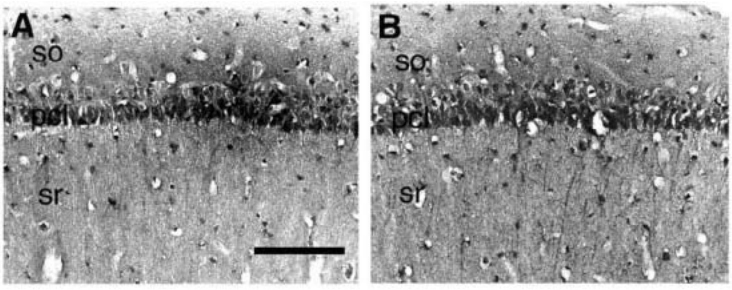

Figure 5

Immunohistochemical staining with antibodies against ADR and ADX in the hippocampal CA1 region of an adult male rat. **A**, ADR; **B**, ADX. so, stratum oriens; pcl, pyramidal cell layer; sr, stratum radiatum. The scale bar indicates 120 μm.

Panel A

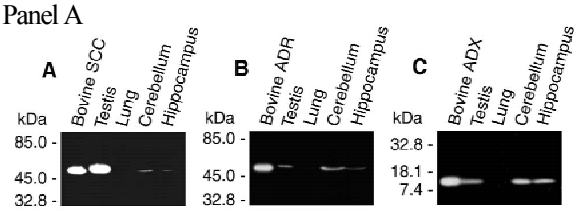

Panel B

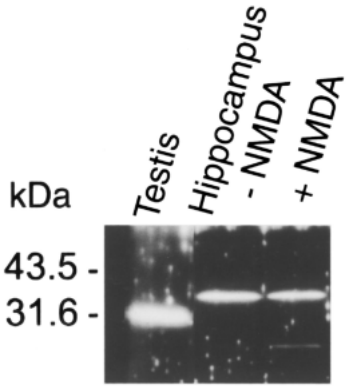

Figure 6

Panel A: Western immunoblot analysis of P450scc, ADR and ADX in the mitochondria from the hippocampus. **A**, P450scc; **B**, ADR; **C**, ADX. From left to right the three panels show purified bovine protein (P450scc in **A**, ADR in **B**, and ADX in **C**), mitochondria from the testis, lung, cerebellum and hippocampus. Rat lung mitochondria are used as a negative control. Panel B: Western immunoblot analysis of StAR from the hippocampal mitochondria. –NMDA, control without NMDA; +NMDA, the hippocampus was stimulated by 100 μM NMDA for 30 min. Not only a thick 37 kDa band but also a weak 30 kDa band appeare on +NMDA. Testis StAR of 30 kDa is used as a positive control.

that the majority of P450scc–containing cells are neither astroglial cells nor oligodendroglial cells. Our careful observation suggested the presence of a slight amount of neurosteroidogenic proteins in glial cells, because of an observed immunoreactivity against P450scc in some glia–like cells.

Neurosteroidogenic activity analysis

We examined the activity of the neurosteroidogenic system in the hippocampus by means of specific radioimmunoassay (RIA) using antibodies against PREG (see Fig 7) (23, 24). The basal concentrations of PREG and PREGS were approximately 0.2– 0.3 pmol/mg protein (i.e., 0.02–0.03 pmol/wet weight, 20–30 nM) which is roughly 10–fold greater than those typical of plasma. In order to demonstrate the acute net production of neurosteroids during neuron–neuron communication, the NMDA–stimulated production of PREG and PREGS was investigated in hippocampal cubic slices. Upon stimulation with 100 μM NMDA for 30 min at 37 deg, the hippocampal level of PREG and PREGS increased to 0.4 – 0.6 pmol per mg of protein, resulting in an increase of about 2– to 3–fold in the basal levels. Stimulation of PREG and PREGS production with NMDA was completely suppressed by either the application of MK–801 and AP–5, which are specific blockers of NMDA receptors, or by the depletion of extracellular Ca^{2+}. This suggestes that NMDA–induced PREG production was mediated by the influx of Ca^{2+} through NMDA receptors. Aminoglutethimide (a specific inhibitor of P450scc) completely blocked the PREG production induced by NMDA stimulation, indicating that the PREG production in the hippocampus was solely due to the P450scc enzyme.

The production of 17β–estradiol was also investigated with RIA using antibodies against estradiol. The basal concentration of estradiol was approximately 0.006 pmol/mg protein (600 pM) which is roughly 6–times greater than that typical of plasma. When the hippocampus was

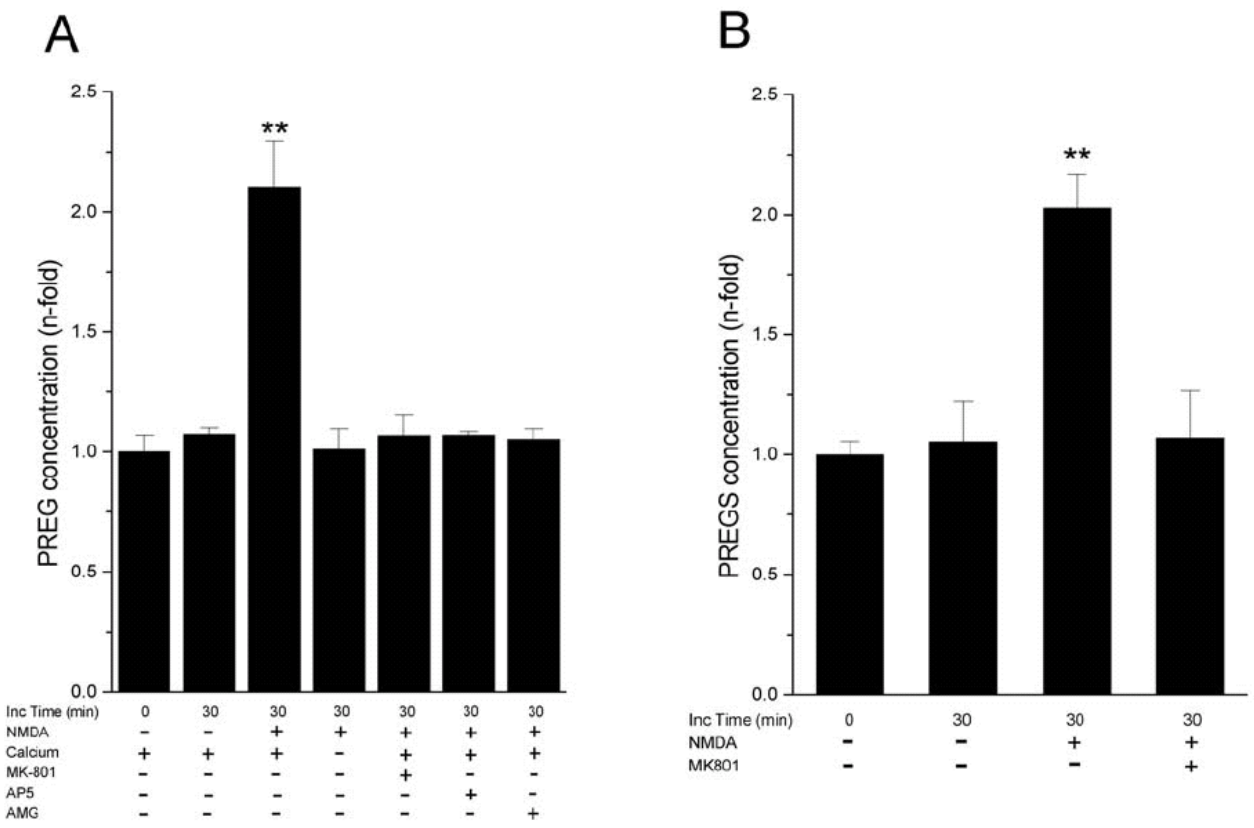

Figure 7

Effect of NMDA–stimulation on neurosteroid synthesis in the hippocampal cubic slices, as measured with RIA. Panel **A**, PREG production; Panel **B**, PREGS production. From left to right in both Panels, basal concentration, 30 min incubation without NMDA, 30 min incubation with 100 μM NMDA, 30 min incubation with NMDA in the presence of blocker MK–801. Vertical scale in each panel is the relative PREG or PREGS concentration normalized by the basal values (0.165 pmol /mg protein for PREG and 0.294 pmol /mg protein for PREGS). Each column represents the mean±SEM of four to seven independent determinations, each analyzed in duplicate. **P<0.01 compared with the PREG or PREGS concentration in the case of the 30–min incubation without NMDA stimulation.

stimulated with 100 μM NMDA for 30 min at 37 deg in the presence of metyrapon (a specific inhibitor of P45011β), estradiol concentration increased to approximately 0.013 pmol/mg protein. In the absence of methyrapon, however, NMDA–stimulation failed to induce an increase in the level of estradiol, suggesting that the estradiol–synthesis pathway is competitive against CORT–synthesis pathway upon stimulation with NMDA.

Synthesis of DHEA and estradiol has also been investigated by means of High Performance Liquid Chromatography (HPLC) analysis. Significant conversion of [^{3}H]–PREG to [^{3}H]–DHEA was observed in the hippocampal cubic slices after incubation for 5 h at 20 deg. When [^{3}H]–PREG was incubated with hippocampal slices in the presence of bifonazole, specific inhibitor of P45017α,, the elution peak of [^{3}H]–DHEA disappeared. When [^{3}H]–DHEA was incubated with hippocampal slices for 5 h at 20 deg, significant amounts of [^{3}H]–androstenedione, [^{3}H]–testosterone and [^{3}H]–estradiol were observed. The approximate relative ratio was androstenedione : testosterone : estradiol = 1:2:17, showing the effective synthesis of estradiol. [^{3}H]–estradiol was formed when [^{3}H]–testosterone was incubated with hippocampal slices for 5 h. These results imply that 17β–estradiol was synthesized from DHEA through androstenedione, testosterone and estrone in the hippocampus. This suggests that the hypothesis, that the conversion of peripheral testosterone to estradiol may be responsible for development of the male type brain from the default female type brain, might not be valid for the hippocampus. It should be noted that the presence of mRNAs

for 17β–HSD type 1 and type 3 was demonstrated in the hippocampus (21). 17β–HSD type 1 and 17β–HSD type 3 catalyze the conversion of estrone to estradiol, and the conversion of androstenedione to testosterone, respectively.

It is important to consider whether the local concentration of neurosteroids is sufficiently high for them to act as local mediators. In order to examine the significance of the concentration of PREGS, we tried to convert the dimensions from pmol / mg protein to M (mol /L). We determined that 10 mg wet weight of the hippocampal tissue contained 0.96 mg of protein. We could assume that tissue having 1mg of wet weight has an approximate volume of 1 μl, because the major part of tissue consists of water whose 1 mL weight is 1 g. The volume may be decreased by only less than 10%, when we consider specific volumes for protein and lipid (about 0.7 – 0.8 ml / g). The basal level of PREGS in the hippocampus is then about 28 nM. After NMDA–stimulation, the concentration of PREGS becomes 57 nM. The local concentration of PREGS in the pyramidal neurons is likely to be 10–20 fold higher than the bulk concentration of 57 nM, due to the relatively small volume of the P450–immunoreactive parts in the total hippocampus. These considerations suggest that the local concentration of PREGS could be as high as 0.6–1.2 μM, which should be sufficient for it to act as a local mediator that modulates NMDA receptors (7, 8). Concerning 17β–estradiol, NMDA–stimulation increased the concentration from 0.6 nM (basal) to 1.3 nM, which is estimated to correspond to a 13–26 nM local concentration within neurons.

1. 2 Action of neurosteroids on NMDA receptors

PREGS and estradiol induce potentiation of NMDA receptor–mediated Ca^{2+} signals

We investigated the NMDA receptor–mediated elevation in the intracellular calcium concentration ($[Ca^{2+}]_i$) with digital fluorescence microscopy, using the Ca^{2+}–sensitive indicator, fura–2 or Calcium Green–1 (32). For isolated hippocampal neurons from 3–day–old rats, cultured 8–10 days, application of 100 μM NMDA induced a transient elevation in $[Ca^{2+}]_i$ which lasted for about 20–60 sec in 86% of the neurons, in the absence of steroids, and in Mg^{2+}–free medium. Preincubation with 100 μM PREGS for 20 min at 37 deg increased the peak amplitude of Ca^{2+} transients by 1.4–fold, as well as increasing the population of NMDA–responsive neurons from 86% to 92%. PREGS did not change considerably the time course of NMDA–induced Ca^{2+} transients. These results, taken together with intracellular electrophysiological measurements combined with NMDA stimulation (10, 33), imply that PREGS increases the opening probability of the NMDA receptor without affecting the mean open time. We also observed a similar enhancement of Ca^{2+} signals upon NMDA application in hippocampal slices by the preperfusion of 50–100 μM PREGS for 20 min.

Estradiol, at a micromolar high concentration, was observed to acutely potentiate the NMDA receptor–mediated Ca^{2+} influx. Preincubation with 10–50μM estradiol for 20 min prolonged the duration of Ca^{2+} signals from 20–60 sec (in the absence of estradiol) to 5–10 min (in the presence of estradiol) without significantly changing the population of NMDA–responsive cells (see Fig. 8, Panel 1). These results indicate that PREGS and estradiol have very different modes of potentiation to NMDA receptors.

PREGS enhances nitric oxide (NO) production

The presence of PREGS enhanced the NO production which was induced upon 1 mM NMDA perfusion in the hippocampal slices (from 4–week–old rat) in Mg^{2+}–free medium at 37 deg. The production of NO was measured as two dimensional images using diaminofluorescein–FM (DAF–FM) whose fluorescence was selectively increased by reaction with NO (34). The perfusion of 100 μM PREGS for 20 min enhanced the NMDA–mediated NO production by approximately 2–fold, especially in the CA1 region (35). On the other hand, the considerable PREGS–induced enhancement of NO production, in relation to Ca^{2+} transients, was quantitatively examined with diaminofluorescein–2 (DAF–2) fluorescence in genetically engineered Chinese hamster ovary (CHO) cells by imaging analysis. We expressed heterologously neuronal NO synthase in a stable transfectant CHO line expressing heat–inducible alleles of NMDA receptors which were mouse GluR ε 1(NR2A) with GluR ζ 1(NR1) subunits or GluR ε 2(NR2B) with GluR ζ 1(NR1) subunits. In contrast to hippocampal neurons, these CHO cells showed a step Ca^{2+} elevation upon only NMDA stimulation (36). Fifty μM PREGS enhanced the NMDA –induced NO production by approximately 1.5–fold. This is in a good coincidence with an approximate 1.5–fold increase in the average Ca^{2+} influx upon NMDA stimulation (see Fig.

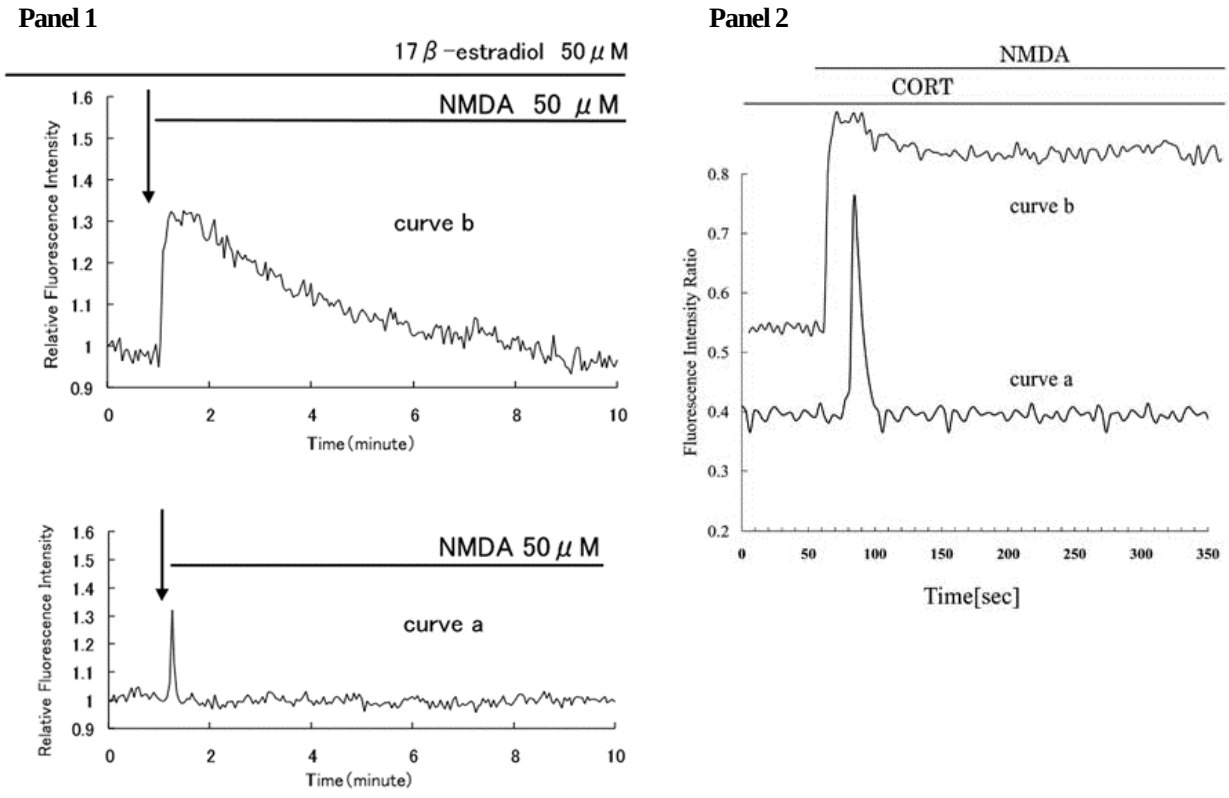

Figure 8

Estradiol and CORT prolonged Ca^{2+} elevation induced upon NMDA stimulation in cultured hippocampal neurons. **Panel 1**: Curve a, the time course of the transient Ca^{2+} elevation induced upon application of 100 μM NMDA. Curve b, preincubation with 50 μM estradiol before NMDA application significantly prolongs the Ca^{2+} elevation. The vertical scale is the normalized relative fluorescence intensity of Calcium Green–1. **Panel 2**: Curve a, the time course of transient Ca^{2+} elevation induced upon application of 100 μM NMDA. Curve b, preincubation with 1 μM CORT before NMDA application extremely prolongs the Ca^{2+} elevation. The vertical scale is the ratio of the fluorescence intensity of fura–2 excited at 340 nm and 380 nm. Curve b in both panels is vertically displaced for illustrative purposes.

9) (37). The increase in the NO production was probably due to PREGS–dependent potentiation of NMDA receptor–mediated Ca^{2+} influx, because the activity of neuronal NO synthase is Ca^{2+}/ calmodulin dependent.

PREGS potentiates the development of long–term potentiation

In the electrophysiological field potential measurements, long–term potentiation (LTP) of CA1 pyramidal neurons is defined as a 1.5–2 fold increase of the initial slope of excitatory postsynaptic potential (EPSP) upon tetanic stimulation of Schaffer collaterals with 100 Hz for 1 sec in the hippocampal slices (from 4–week–old rats) with 1 mM of Mg^{2+} at 30 deg. The 30 Hz for 1–sec tetanic stimulation, however, did not induce LTP. Preperfusion with 100 μM PREGS for 10 min considerably increased the EPSP slope by approximately 1.4–fold upon stimulation with 30 Hz (see Fig. 10), indicating the LTP–development. Interestingly even without tetanic stimulation in 1 mM Mg^{2+} medium, the perfusion of 10-100 μM PREGS for only 2 min increased both the slope and the peak magnitude of EPSP by approximately 1.8–fold. This enhancement of EPSP lasted stably during the perfusion of PREGS. The LTP–induction by PREGS is probably due to the potentiation of NMDA receptor–mediated Ca^{2+} currents by PREGS (10, 33). Because PREGS is known to suppress AMPA type of glutamate receptors, the enhancement of LTP–induction implies that the potentiation of NMDA receptors overcomes

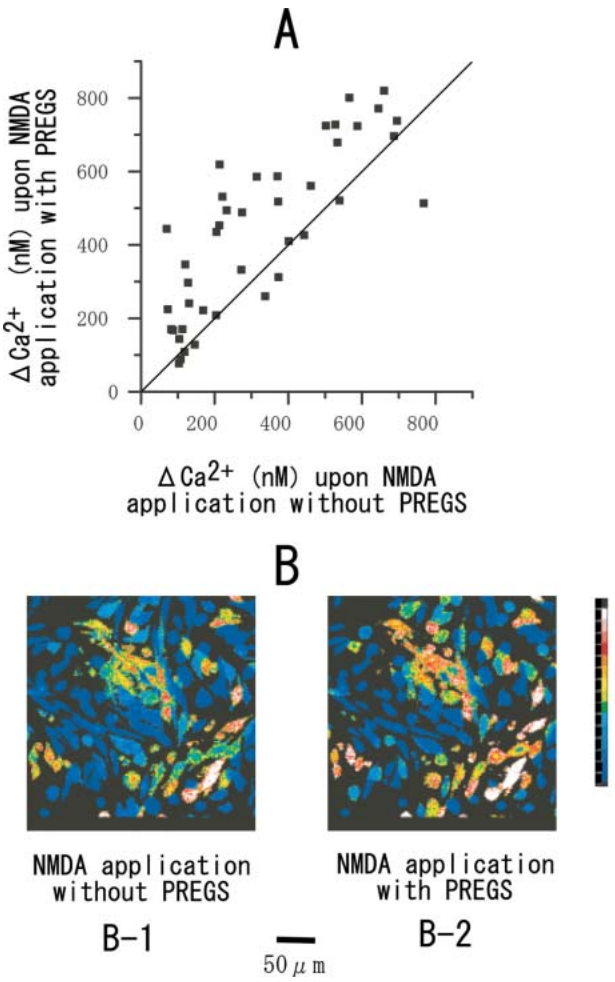

Figure 9

PREGS potentiated NMDA–induced Ca^{2+} elevation through genetically expressed ε 2/ ξ 1 NMDA receptors in CHO cells. **Panel A**: Plot of intracellular Ca^{2+} elevation (ΔCa^{2+}) upon NMDA application in the presence vs. in the absence of 50 μM PREGS for the same single cells. Vertical axis is the Ca^{2+} elevation (ΔCa^{2+}) in the presence of PREGS and the horizontal axis is ΔCa^{2+} in the absence of PREGS for the same cells. First, cells were stimulated by 100 μM NMDA perfusion without PREGS, then NMDA was wash out, resulting in Ca^{2+} decrease to the resting level. Second, the same cells were perfused with 50 μM PREGS for 20 min, followed by a perfusion of 100 μM NMDA with 50 μM PREGS for stimulation. **Panel B**: Pseudocolored images demonstrate that CHO cells expressing ε 2/ ξ 1 NMDA receptors show Ca^{2+} elevation upon 100 μM NMDA stimulation, in the absence of PREGS (**B–1**), and in the presence of PREG (**B–2**). The ratio of fura–2 fluorescence is indicated with a color bar. Scale bar is 50 μm.

the suppression of AMPA receptors in synaptic signal transduction.

Effect of estradiol on the induction of long–term potentiation

Complex results were observed for the acute effect of estradiol in developing the LTP of CA1 pyramidal neurons. When 100 Hz for 1 sec tetanic stimulation of Schaffer collaterals was applied, the preperfusion of 0.1–10 nM estradiol for 20 min reduced the induction of LTP of the slice from 4–week–old rat as indicated by an approximate 1.3–fold enhancement of the EPSP slope (our results; ref. 14), while the preperfusion of estradiol did not affect the induction of LTP of the slice from adult rat (3 month-old) (14). When theta-burst stimulation (e.g., 100 Hz for 200 msec, 10 sec intervals, 5 times applications) was applied to the slice from adult rat, the preperfusion with 0.1–10 nM estradiol for 20 min was alternately effective in developing LTP as indicated by an approximate 2–fold enhancement of the slope and the peak magnitude of EPSP (13), or ineffective in induction of LTP as indicated by almost no enhancement nor depression on the slope and the peak magnitude of EPSP (K. Ito, personal communication). When the NMDA receptor–mediated EPSP was measured in a low Mg^{2+} medium (100 μM Mg^{2+}), the magnitude of EPSP was considerably enhanced under the preperfusion of 0.1–100 nM estradiol (our results; ref. 13). Further experiments should be performed to resolve these complicated effects of estradiol on neuron–neuron communication.

Corticosterone acutely and extremely prolongs NMDA receptor–mediated Ca^{2+} elevation in cultured hippocampal neurons

Corticosterone (CORT) is a principal glucocorticoid that is synthesized in the rodent (e.g., rat and mouse) adrenal cortex and secreted in response to stress. Note that more cortisol than CORT is produced in primates such as the

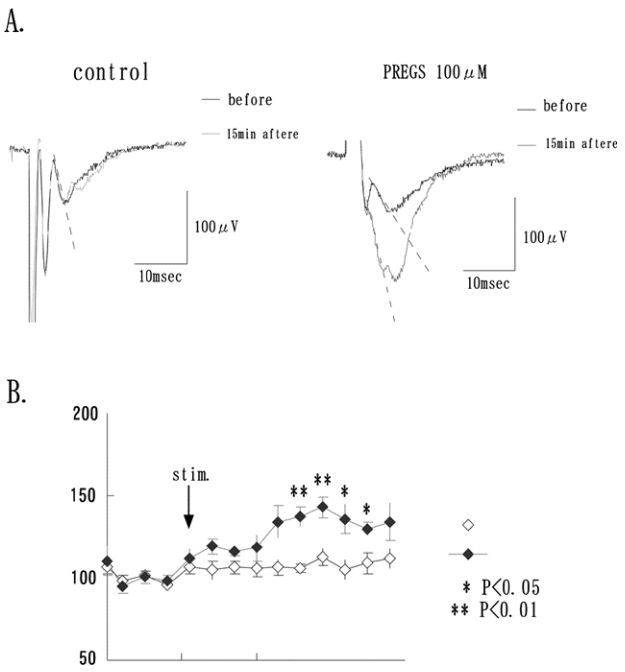

Figure 10

Enhancement of LTP–development by preperfusion of PREGS for 30 min in hippocampal slices. Panel A: Left, In the absence of PREGS. EPSP before the 30 Hz stimulation and EPSP at 15 min after the stimulation. Right, In the presence of PREGS. EPSP before the 30 Hz stimulation and EPSP at 15 min after the stimulation. Panel B: Time–dependence of the EPSP slope with PREGS (blue filled square) and control EPSP slope without PREGS (black open square). The slope of the EPSP increases by roughly 1.4–fold upon 30 Hz tetanic stimulation for 1 sec, after the preperfusion of 100 μM PREGS for 30 min, whereas the slope is not significantly changed in the absence of PREGS.

humans. To date, little had been known about the acute effects, which appear within 30 min, of CORT on neurotransmitter-mediated signal transduction in hippocampal neurons. We therefore examined the acute effects of CORT using digital fluorescence microscopy, with the Ca^{2+}–sensitive indicator, fura –2.

CORT induced an acute effect on NMDA receptor–mediated Ca^{2+} signaling at 37 deg in cultured hippocampal neurons isolated from 3–day–old rats (32). We observed that CORT modulated the NMDA receptor–mediated elevation in $[Ca^{2+}]_i$ completely differently from PREGS in the hippocampal neurons. By preincubation of neurons with 0.5–50 μM CORT for 20 min in the absence of extracellular Mg^{2+}, NMDA induced an extremely prolonged Ca^{2+} elevation which was never terminated over the experimental time range of 5–20 min (Fig.8 Panel 2). Blocking NMDA receptors by MK801 terminated the prolonged $[Ca^{2+}]_i$ elevation. CORT did not increase the population of the NMDA–responsive neurons. The very prolonged $[Ca^{2+}]_i$ elevation by the presence of CORT caused the loss of mitochondrial membrane potential, as observed with rhodamine 123. These results imply that a high concentration of CORT (>0.5 μM), possibly secreted during stress, acutely inhibited the closing of NMDA receptors which were once opened by NMDA, and resulted in a Ca^{2+}–dependent neurotoxicity in the hippocampus.

CORT acutely suppresses LTP–induction

The LTP of CA1 pyramidal neurons was induced upon high–frequency stimulation of Schaffer collaterals with 100 Hz for 1 sec in the hippocampal slices in the presence of high concentration (1 mM) Mg^{2+} at 30 deg, as determined by an increase in the EPSP slope by approximately 1.5–fold. Preperfusion with 10 μM CORT for 20 min considerably suppressed the LTP–development, reducing the increase in the EPSP slope to 1.2–1.3 fold upon the 100 Hz tetanic stimulation. The suppression of LTP–development in the presence of CORT might be due to an extremely enhanced Ca^{2+} influx through NMDA receptors during a 1–sec tetanic stimulation, as judged from the Ca^{2+} measurements of cultured hippocampal neurons. Our findings suggest that the suppression of LTP–development would occur acutely (<30min), as a result of a stressful concentration of CORT in vivo. Until our study, by the observation of delayed genomic effects requiring 5–24 h, high levels of glucocorticoids were shown to inhibit LTP induction and to impair learning (38–40). By the way, where does CORT come from? Does CORT reach the brain only from the adrenal glands? CORT synthesis from [^{3}H] –deoxycorticosterone and the presence of mRNAs of P450c21 and P45011β have been reported in the rat hippocampus (22). Although the evidence is not conclusive, during stressful situations, the hippocampus itself might synthesize a high concentration of CORT which then acutely suppresses neuron–neuron communication as well as peripheral CORT supplied from the adrenal glands.

On the other hand, a series of studies about chronic and genomic effects of corticosteroids in the hippocampus has

been reported (41, 42). Stress–induced increase in CORT secretion was shown to produce neuronal cell damage. Exogenous application of a high dose of CORT endangered the neurons in the hippocampus (43, 44). Three weeks of treatment with CORT lead to neuronal atrophy selective for CA3 pyramidal neurons in the hippocampus. Rats exposed to restraint stress for 3 weeks exhibited neuronal atrophy identical to that seen in rats treated with high–dose CORT for 3 weeks (45). So far, investigations on rapid modulation of hippocampal neuronal activities by adrenal steroids have been quite exceptional. Most studies performed over the past few decades show that glucocorticoids exert delayed, conditional actions on hippocampal activity (46).

Discussion on neurosteroids

Our results shed light on the physiological reality of neurosteroids as local mediators concerning the site where they are synthesized, and where and how they act.

So far, many works have reported the absence of P45017α, in the brain. Therefore, it has been believed that DHEA and testosterone may be supplied by blood circulation, resulting in the conversion to estradiol in hypothalamus and amygdala where P450arom is expressed. Gonadal sex steroids and DHEA had not been realized as neurosteroids, because their synthesis had not been demonstrated in the brain. Only PREG(S), pregnanolone, allopregnanolone and allotetrahydrocorticosterone have been supposed to be 'true' neurosteroids (6). Even progesterone had not been included in neurosteroids. Our discovery of the NMDA–dependent machinery of estradiol–synthesis, starting from domestic cholesterol to estradiol and testosterone through DHEA, introduces an essentially a new class of neurosteroids, having a new role in the process of signal transduction in the brain.

Our experimental knowledge, taken together indicates that PREGS causes postsynaptic signal amplification, as illustrated in Fig. 11. In particular, an NMDA–gated Ca^{2+} influx triggers a cascade of steroidogenesis by StAR and P450scc. This increases the production of PREG and PREGS, which in turn potentiates an NMDA receptor–mediated Ca^{2+} influx. By this means, PREGS facilitates the excitation of neurons at the postsynaptic level. The production of PREG and PREGS in the hippocampus was found to be enhanced by approximately 2–fold upon stimulation with NMDA, strongly suggesting positive feedback between NMDA receptor activation and the production of PREGS. This possible acute (<30min) postsynaptic signal amplification through a "PREGS → NMDA receptor → Ca^{2+}" cycle might directly contribute to the LTP of hippocampal pyramidal neurons, in which PREGS acts as a mediator of the postsynaptic LTP–development. Our first observation of the enhancement in LTP–induction by PREGS in the CA1 pyramidal neurons strongly supports this hypothesis.

The acute action (<30min) of estradiol on glutamate-mediated neuronal excitability is complex. Although the production of estradiol was enhanced by the NMDA–gated Ca^{2+} influx, this increase of estradiol may acutely suppress the LTP–induction. When a 100 Hz for 1 sec tetanic stimulation was applied, a pretreatment of 0.1–10 nM estradiol suppressed the development of LTP for 4 week-old rats. On the other hand, upon theta-burst stimulation (100 Hz for 200 ms, 5 times with 10 sec interval), a preperfusion of 0.1–10 nM estradiol potentiated the development of LTP (13), or no effect on development of the LTP for adult rats (14, personal communication). Note that a preperfusion of 0.1–10 nM estradiol for 10 min potentiated the population spike amplitude which has close relation to action potential (12), implying that the effect of estradiol is different between glutamate-gating and voltage gating Ca^{2+} channels.

Our essential contribution is the discovery of a paracrine supply of estradiol from an NMDA–dependent neuronal machinery which synthesizes estradiol from domestic cholesterol, suggesting that the supply of peripheral gonadal steroids by blood circulation may not play a central role in modulating rapid neuron–neuron communication. Because one year therapy with 17β–estradiol for female patients of Alzheimer's disease after menopause was very effective in improving their capacity for leraning and memory (47), our finding of neuronal synthesis and acute action of estradiol may serve as a molecular basis for understanding its therapeutic effects. Acute effect of estradiol also includes MAP kinase–dependent cell protection in which membrane estradiol receptors are considered to be involved (48). For example, estradiol was demonstrated to protect the degradation of hippocampal NMDA receptors by only 10 min exposure (49). On the other hand, we propose the other type of modulation for CORT in neuronal communication. In stressful situations, a high level of CORT (cortisol in the case of primates), either produced in the hippocampus or coming

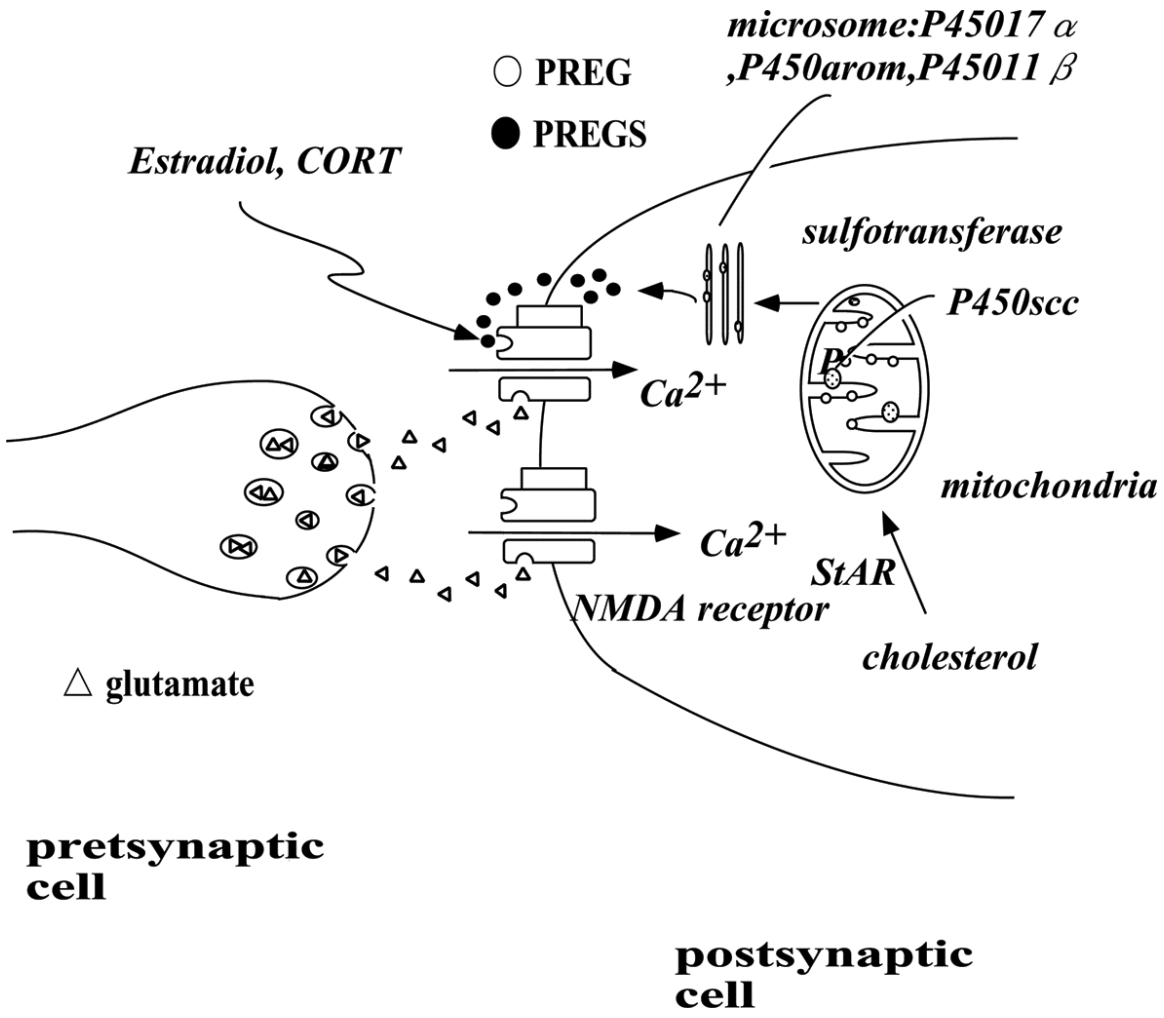

Figure 11

A possible postsynaptic signal amplification cascade mediated by PREGS in the hippocampus: NMDA–gating Ca^{2+} influx → StAR transports cytosolic chole onverts cholesterol to PREG →convertion to PREGS → potentiation flux → StAR → P450scc → .....

Possible modulation by PREGS, estradiol and CORT may be performed (1) by their direct binding to NMDA receptors or (2) via binding to their specific membrane receptors, followed by interactions with NMDA receptors. For illustrative purposes, AMPA type of glutamate receptors are omitted.

from the adrenal glands, extremely prolongs the NMDA receptor–mediated Ca^{2+} elevation, and results in the suppression of LTP–development.

It should be noted that NMDA receptor–dependent LTP corresponds to the synaptic mechanism of memory, because selective NMDA antagonists delivered to the brain impairs hippocampus LTP. NMDA–dependent strengthening of CA1 synapses is demonstrated to be essential for the acquisition and storage of spatial memory of transgenic mice in which the NMDA receptors had been selectively deleted in the CA1 pyramidal cells (50, 51).

Prior to our extensive investigations, there were few reports which demonstrated the specific cellular distributions of steroidogenic proteins in the cerebrum. In the rat cerebellum, the neuronal localization of P450scc was demonstrated in Purkinje neurons and granule cells by immunohistochemistry (52). A significant amount of PREG was observed in the whole cerebellum. PREGS was observed to enhance the electrical activity of Purkinje neurons, may be due to suppressing GABA neurons (53). Neuronal expression of the P450scc mRNA was reported in other rat nervous systems, such as neurons in the retinal ganglion, sensory

neurons in the dorsal root ganglia, and primary cultures of rat cerebellar granule cells (18, 19, 54). In the isolated rat retina, the concentrations of both PREGS and PREG were almost the same (approximately 0.5 ng/mg protein) (55). NMDA–induced enhancement of the production of PREG and PREGS was also demonstrated in the retina, with approximately a 2–fold enhancement (55, 56).

The specificity of steroid–binding and modulation on NMDA receptors should be examined. PREGS, estradiol and CORT has been observed to modulate NMDA receptors very differently. The copresence of progesterone with CORT completely prevented the modulation effect of CORT. The observed effects, therefore, cannot be nonspecific ones caused by the membrane–solvation of steroids or membrane–disordering by steroids. The specificity of these steroid effects for NMDA receptors may not be lower than that for GABA receptors because more than a micromolar concentration range of PREGS was also necessary to modulate GABA receptors specifically. Note that PREGS and DHEA have specific, high affinity binding sites on GABA receptors (56-59). There is, however, a possibility of the existence of novel membrane receptors for neurosteroids which differ from NMDA receptors, particularly for estradiol, because the application of 1–100 nM estradiol alone without NMDA acutely produces Ca^{2+} transients in the cultured rat hippocampal neurons, glial cells (60) and embryonic midbrain dopaminergic neurons (61). It should be noted that the application of estradiol alone did not produce Ca^{2+} transients in CHO cells genetically expressing NMDA receptors.

In a classical view of steroid hormone actions, steroids have been considered to require binding to intracellular nuclear steroid receptors after reaching neurons by circulation. Because activation of both the transcriptional and translational machinery of the cells is necessary for the classical steroid actions, there must be a time–lag of hours to days between the beginning of the actions and their physiological consequences.

The influence of steroids on memory storage in the hippocampus has attracted much attention in behavioral studies. Peripheral steroids may influence memory processes by modulating LTP in the hippocampus, which has recently been shown to be inhibited by high–stress–induced levels of glucocorticoids and to be chronically enhanced by low endogenous levels (41). With regard to delayed genomic effects, it is still unknown why stress–elevated high levels of glucocorticoids enhance Ca^{2+} conductance and cause neuronal atrophy in CA3 pyramidal neurons in the hippocampus. The blockade of NMDA receptors and the suppression of glutamate release were effective in inhibiting neuronal atrophy (62). Our finding of a CORT–induced, stable open state of NMDA receptors might also explain the chronic, Ca^{2+}–dependent neurotoxicity in the hippocampus. Another open question is why neuronal atrophy selectively occurs in CA3 pyramidal neurons but not in CA1. One possible explanation is that CA3 neurons lack Ca^{2+}–binding proteins which are abundantly contained in CA1 neurons, such as calbindin D28k and parvalbumin (63).

Chap. 2 Mechanisms of steroid synthesis in the adrenal cortex

Introduction

Mechanisms of steroidogenesis have been extensively investigated in adrenocortical cells which are much more enriched in steroidogenic enzymes than brain cells (64). Peripheral steroid hormones produced in adrenocortical cells play a key role in gluconeogenesis in the liver, homeostasis of Na^+ /K^+ concentration, and suppression of inflammation. The rate of steroid hormone synthesis is rapidly (5–20 min) increased upon hormonal stimulation of adrenocorticotropic hormone (ACTH) in adrenal fasciculata cells (65). Upon ACTH stimulation, signal transduction appears to occur sequentially in the following manner. ACTH binds to the hormone receptors in the plasma membrane, which triggers Ca^{2+} signals or cAMP signals in the cytoplasm. This in turn stimulates the conversion of cholesterol to PREG by P450scc in the mitochondria. A successive hydroxylation of steroids then occurs in microsomes and mitochondria, which results in corticoid production (see in Fig.1 and Fig. 2). A flow of steroid metabolism is as follows: PREG → progesterone → deoxycorticosterone → CORT. Concerning cholesterol mobilization, cholesterol in the inner mitochondrial membrane may first be utilized rapidly (< 5 min) by P450scc, and then supplied from the outer to the inner membrane (~20 min) by StAR or peripheral benzodiazepin receptors (66). Cholesterol supply from the cytoplasm would be much

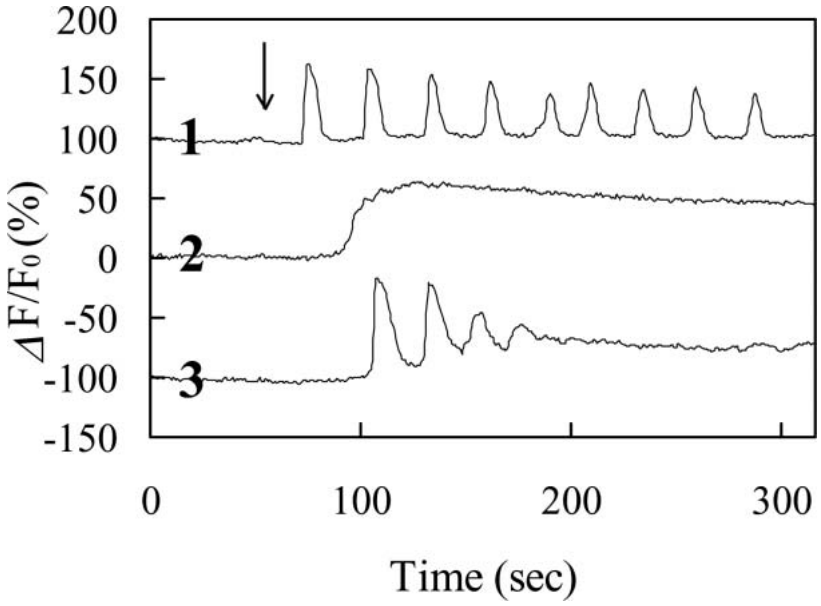

Figure 12

The time course of typical Ca^{2+} signaling induced by 1 pM ACTH in cultured adrenocortical cells. Curve 1, Ca^{2+} oscillations; curve 2, step–like increase in Ca^{2+} ; curve 3, Ca^{2+} oscillations superimposed on the step–like increase in Ca^{2+}. The vertical scale ($\triangle F/F_0$) is the ratio of the fluorescence intensity change ($\triangle F = F–F_0$) to the basal fluorescence, F_0.

slower.

The identity of physiological second messengers for ACTH action has been controversial for a long time. It had been believed that cAMP is a major second messenger, because cAMP synthesis in the adrenal cells was stimulated by pharmacological concentrations of ACTH (100 pM–1 μM) and the application of cAMP analogs activates adrenal steroidogenesis (67). In the presence of a 1–50 pM concentration of ACTH (i.e., the physiological level of ACTH), however, steroidogenesis was stimulated but cAMP synthesis was not increased significantly (68). Ca^{2+} ions play an important role in steroidogenesis, because their removal or the addition of calcium channel blockers is known to reduce or abolish the corticoid response. We therefore challenged to demonstrate that ACTH induce a direct Ca^{2+} signaling, which drives a cascade of enzyme reactions downstream. In order to investigate the important elementary steps of steroidogenesis reactions at a molecular level, we have employed digital fluorescence microscopic imaging for P450 activity and cholesterol trafficking.

2. 1 Imaging of calcium signaling

With fluorescence microscopic imaging, we have discovered that Ca^{2+} signaling occurrs in Calcium Green–1 –loaded bovine adrenal fasciculata cells upon stimulation with ACTH, at a physiological concentration of 1–100 pM (69). Because it was very difficult to achieve good loading of adrenocortical cells with calcium indicators, we used a high concentration of Cremophore of 0.03% in order to obtain complete dissolution of Calcium Green–1/AM during cell loading (70). More than 90% of the fasciculata cells was therefore loaded in 10–min incubation at 37 deg with 3 μM Calcium Green–1/AM.

We observed three patterns of Ca^{2+} signaling: Ca^{2+} oscillations with a frequency around 0.04 Hz (33%), a step–like increase in Ca^{2+} concentration (10%), and Ca^{2+} oscillations superimposed on a step–like increase in Ca^{2+} (57%) (Fig. 12). The Ca^{2+} oscillations induced by ACTH were almost completely suppressed by the addition of EGTA (to deplete Ca^{2+} in the outer medium) and thapsigargin (to inhibit Ca^{2+} release from microsomes). When the Ca^{2+}

signaling was inhibited by the treatment with EGTA, the corticoid production during 60 min was considerably suppressed to 11 % of that of cells stimulated with 100 pM ACTH (69). Note that stimulation with 100 pM ACTH increased the corticoid production by 12–fold over that of control non–stimulated cells (551 pmol of corticoid/10^6 cells/hr). These results suggest that the Ca^{2+} signaling is a second messenger for ACTH–induced steroid hormone synthesis in zona fasciculata cells. To confirm this, we used NPS–ACTH, an ACTH analogue which induces Ca^{2+} signaling with no accompanying cAMP production, even at 1mM NPS–ACTH. NPS–ACTH increased both the PREG production and the population of Ca^{2+} signaling cells (71).

2.2 Real–time analysis of the activity of P450scc, using a fluorescent cholesterol analogue

The catalytic activity of P450scc is normally measured with RIA to detect pregnenolone production. RIA does not have good time resolution, and we cannot analyze at the single cell level. To investigate the time dependency of the activity of cytochrome P450scc in real–time, we measured the side–chain cleavage reaction, using 3β-hydroxy-22, 23-bisnor-5-cholenyl ether (cholesterol-resorufin) as a substrate, by observing the distinct increase in fluorescence attendant upon conversion of cholesterol-resorufin to resorufin and pregnenolone. Time-dependent fluorescence analysis with a fluorometer revealed that the activity of P450scc was dependent on cytosolic Ca^{2+} signals arising from extracellular NADPH, ACTH and ATP stimulation in bovine adrenocortical fasciculata cells (72). Cholesterol–resorufin in DMSO was loaded into cultured cells in order to incorporate this substrate analogue into intracellular mitochondria. The resorufin production in adrenocortical cells was completely suppressed by the presence of aminoglutethimide, a specific inhibitor of P450scc, which indicated that the fluorescence increase was due solely to the P450scc side–chain cleavage activity.

The application of extracellular NADPH, 50 –500 μM, was observed to increase both the level and rate of resorufin production in intact cells (see Fig. 13). This extracellular NADPH stimulation was prevented by the addition of thapsigargin and EGTA, which abolished Ca^{2+} oscillations induced by extracellular NADPH. The addition of suramin, a specific antagonist of the P2y type of ATP receptors, also completely abolished the extracellular NADPH–induced

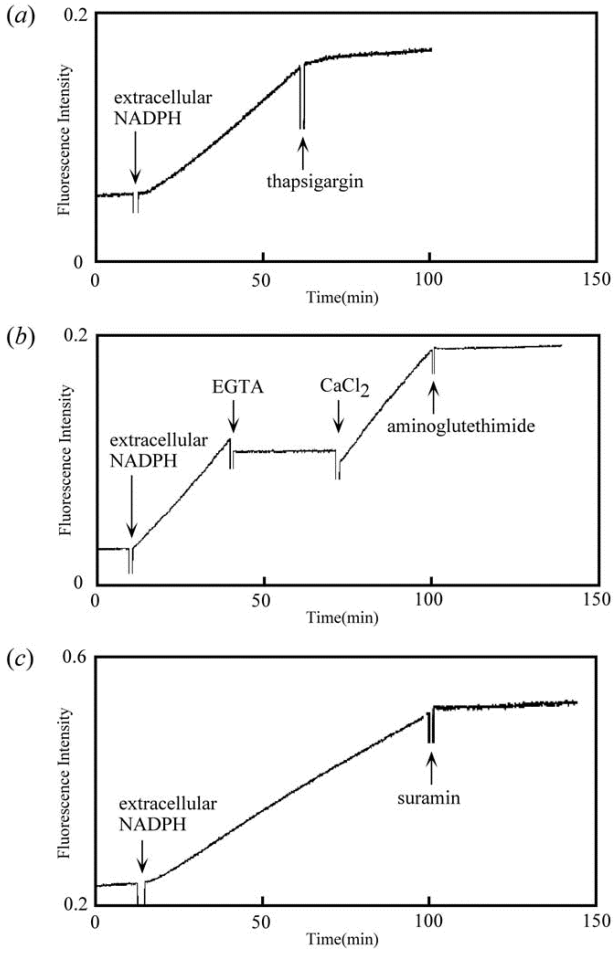

Figure 13

The time–course of the side–chain cleavage activity of P450scc for cholesterol–resorufin in cell suspensions. Panel (a): 10 μM thapsigargin inhibited the P450scc activity induced by extracellular application of 50 μM NADPH. Panel (b): 2 mM EGTA inhibits but extracellular Ca^{2+} supplementation stimulates the P450scc activity induced by 500 μM extracellular NADPH. 100 μM aminoglutethimide inhibits the activity completely. Panel (c): 100 μM suramin suppresses completely the P450scc activity induced by 500 μM extracellular NADPH. Vertical axis is the fluorescence of resorufin. Arrows indicate the time of addition of chemicals.

cholesterol–resorufin conversion. These results imply that extracellular NADPH (membrane impermeable) produced Ca^{2+} oscillations via binding to ATP receptors, thereby stimulating the activity of P450scc. On the other hand, ACTH induced a relatively small increase in the P450scc activity for cholesterol–resorufin. A significant production of resorufin

was observed after stimulation of cell cultures with 100 pM, 1 nM of ACTH for 3 hours. The application of 45–500 μM extracellular ATP to cells did not significantly increase the resorufin production.

The addition of these three stimulators produced very different types of Ca^{2+} signals: The Ca^{2+} signals induced by NADPH was characterized predominantly by a series of Ca^{2+} spikes, without elevation of the basal Ca^{2+} concentration; ACTH induced dominantly a series of Ca^{2+} spikes, superimposed on a long–lasting basal Ca^{2+} elevation; Extracellular ATP induced only a long–lasting Ca^{2+} elevation. The mode of stimulation of cytochrome P450scc may thus be correlated with the different patterns of cytosolic Ca^{2+} signals, although the activity of P450scc should be dependent on mitochondrial Ca^{2+} rather than cytosolic Ca^{2+}.

The NADPH–induced enhancement of cholesterol–resorufin may be achieved by means of stimulation of electron transfer to P450scc by effective penetration of Ca^{2+} oscillations into the mitochondria where Ca^{2+}–dependent NADPH generation systems are present. Although we still do not have direct evidence for this hypothesis, some support is lended by the reported behavior of bovine adrenocortical glomerulosa cells upon stimulation with angiotensinII and ACTH (73, 74). At 100 pM, angiotensinII induced Ca^{2+} oscillations while a step Ca^{2+} elevation was induced at 3 nM. The time course of the increase in intracellular NAD(P)H was coincident with the time –dependent change in the cytosolic Ca^{2+} concentration induced by angiotensinII(75). The coincident change in mitochondrial Ca^{2+} with the change in cytosolic Ca^{2+} was demonstrated using chemiluminescent aequorin, expressed in the mitochondria (73). ACTH–induced Ca^{2+} signals may activate StAR which transports endogenous cholesterol into mitochondria. Our results suggest, however, that StAR may not transport exogenous cholesterol–resorufin, resulting in a rather weak stimulation by ACTH of resorufin production.

2.3 Imaging of trafficking of LDL–containing endosomes

Uptake and transport of cholesterol is essential as the substrate supply for steroidogenesis in adrenocortical cells. Cholesterol uptake is performed by receptor–mediated endocytosis of low density lipoprotein (LDL) bearing cholesterol, and is followed by the trafficking of endosomes containing LDL. To investigate the real–time intracellular trafficking of endosomes, microscopic images were recorded on video tape and analyzed by digital image processing.

LDL was fluorescently labeled with dioctadecyl tetramethyl–indocarbocyamine perchorate (DiI) and applied to adrenocortical fasciculata cells. Approximately 20 min after the pulsed application of LDL to cells, middle endosomes of 0.5 –1 μm in diameter were formed. A digital tracing of single endosomes demonstrated that individual middle endosomes showed rapid forward/backward/immobile movements over short distances, with frequent changes in direction (see Fig. 14). At 60 min after LDL addition, roughly 38% of the endosomes showed rapid and directional movement at a rate of 0.05 – 0.25 μm/sec, with the time range of 72 sec tracing. The remaining 62% of the middle endosomes were temporarily immobile. When the tracks of many endosomes were averaged over several hours, the averaged motion showed very slow perinuclear movement at a velocity of 5–7 μm/h. This very slow velocity is due to frequent changes in the direction of endosome movement. At 3 h after LDL addition, the middle endosomes showed significant concentration around the circumference of the cell nuclei. This is consistent with the very slow velocity of averaged perinuclear motion obtained from single endosome tracking. Nocodasole inhibited the perinuclear movement of middle endosomes by depolymerizing microtubules, which implies that the endosomes underwent directed movement along the microtubule networks. The incorporation of both anti–dynein antibodies and 10–50 μM vanadate into cells by the saponin treatment enhanced the peripherally–directed motion of the endosomes, probably due to the inhibition of perinuclear motion by dynein–like motor proteins (see Fig. 14). In contrast, application of anti–kinesin antibodies induced the facilitated perinuclear concentration of endosomes, probably due to inhibition of peripherally–directed motion by kinesin–like motor proteins. These results indicate that both dynein–like and kinesin–like motor proteins bind to the same endosome, resulting in alternating perinuclear and peripherally–directed movements. Because the number of kinesin–like motor proteins may decrease in LDL–endosomes during perinuclear movement, due to the usage of kinesin–motor proteins for peripherally–directed moving endosomes (including LDL receptors for the recycle), the averaged motion of endosomes had a perinuclear appearance.

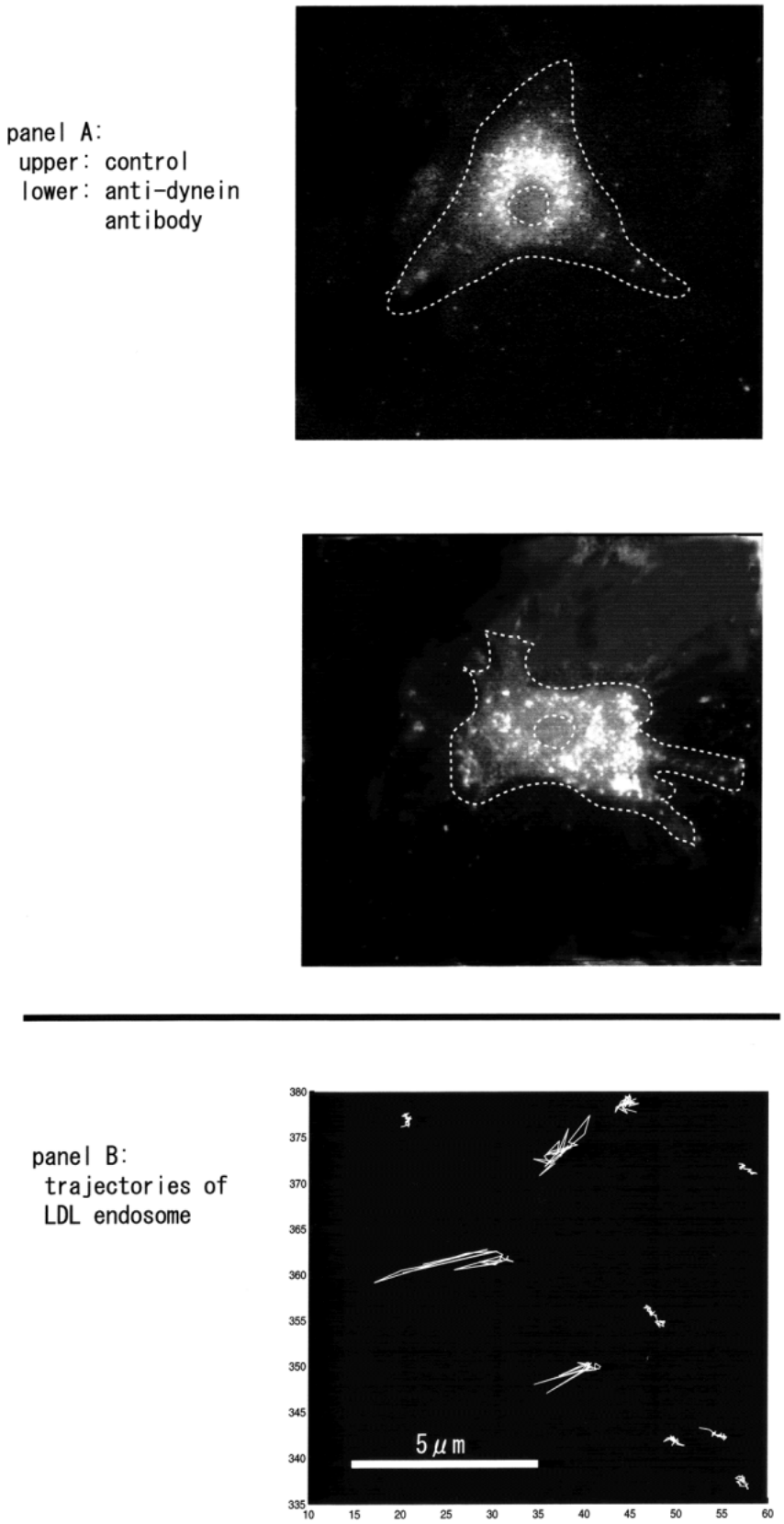

Figure 14

Panel A: The effect of antibody against dynein on the endosome movement.

Upper, Control distribution of endosomes at 3h after the LDL addition. Lower, Peripherally–located distribution of endosomes caused by the addition of anti–dynein antibody which was incorporated into cells at 1 h after the LDL addition, and cells were further incubated for 2 h. Panel B: Trajectories of the middle endosomes are drawn by tracing endosomes for successive 60 images (72 sec) at a time interval of 1.2 sec. These images were taken at 1 h after the LDL addition. The edge of the cell nucleus is placed at the lower right corner.

In adrenocortical cells, the application of ACTH caused a considerable facilitation in the perinuclear motion of the endosomes, resulting in the complete concentration of endosomes around the nuclei within 1 h. ACTH–induced Ca^{2+} signaling is responsible for increasing perinuclear motion by modulating the dynein/kinesin motors, because

depletion of extracellular and/or intracellular Ca^{2+} abolished the ACTH–induced facilitation in the perinuclear motion of the endosomes, probably due to suppression of Ca^{2+} signals induced by ACTH. This may contribute to an acute increase in steroid hormone production induced upon application of ACTH.

We also investigated endosome trafficking in rat cerebral astroglial cells (76). The mechanism of endosome motion was almost the same as that observed in adrenocortical cells except that the rate of averaged perinuclear movement was much slower in astroglial cells than in adrenocortical cells. As a result, 6 h was needed to achieve a significant concentration of endosomes around nuclei. The LDL–containing endosomes underwent rapid forward/backward/immobile motions, with frequent changes in direction. From investigations using anti–dynein and anti–kinesin antibodies, the same endosomes were shown to contain both dynein–like and kinesin–like motor proteins, which resulted in alternative perinuclear and peripherally–directed motions along microtuble networks. The rate of individual endosomes demonstrated qualitatively the same distribution (0.05–0.25 μm/sec) as that in adrenocortical cells.

We investigated the flexible motion of the LDL–bearing LDL receptors in endosomes in adrenocortical cells. Phosphorescence anisotropy r(t) demonstrated that eosin–ITC labeled LDL, bound to the LDL receptors, showed a wobbling motion within a cone of half–angle roughly 60 deg; with a rotational relaxation time of 40 μsec. The measurements were performed at 4 deg, 40 min after the LDL incorporation into cells.

Chap. 3 Electron transfer interactions and membrane topology of cytochrome P450s analyzed by protein rotation measurements

As is shown in Figures 1 and 2, after the conversion of cholesterol to pregnenolone by the ADR+ADX+P450scc system in the mitochondria, PREG is transported to the microsomes where cytochrome P450–containing monooxygenase systems carry out the biotransformation of PREG to various steroid hormones (64). Cytochrome P45017α, accepts electrons from P450 reductase, catalyzing 17α,–hydroxylation of PREG. Cytochrome P450c21 (CYP21) accepts electrons from the reductase, catalyzing 21–hydroxylation of progesterone.

3.1 Adrenocortical mitochondrial P450scc

To investigate a possible ternary association of ADR + ADX + P450scc, we measured the rotational mobility of ADR and ADX upon crosslinking P450scc molecules by antibodies against P450scc in liposomes. ADR and ADX were added exogenously to liposomes containing P450scc which was incorporated into phosphatidylcholine (PC) /phosphatidylethanolamine (PE)/cardiolipin (CL) = 4/4/1 (w/w) vesicles by cholate dialysis procedures. The lipid–to–P450scc ratio was 1: 2 (w/w) and the ADR: ADX: P450scc ratio was 1:1:1 (mol/mol). ADX and ADR were labeled with erythrosin derivatives (ADX with erythrosin–ITC and ADR with erythrosin–IA). Rotational diffusion of ADR/ADX was then measured by observing the decay of phosphorescence anisotropy, r(t), of erythrosin at 3 deg. ADX showed a rapid wobbling with a rotational relaxation time, ϕ, of approximately 20 μs when bound to cytochrome P450scc in the membrane. The addition of ADR to this system significantly decreased the wobbling mobility of ADX. ADR moved rapidly (ϕ of approximately 35 μs) on the membrane surface of liposomes containing ADR, ADX and cytochrome P450scc. Cross–linking of P450scc by anti–P450scc antibodies resulted in a significant decrease in the mobility of both ADR and ADX in ADR+ADX+P450scc liposomes (see Fig.15). It should be noted that the rotation of cytochrome P450scc was very slow (ϕ of approximately 830 μs) in the proteoliposomes at 3 deg. Taken together with biochemical experiments, it is concluded that roughly 10% of the ADR forms a transient ternary association with ADX and P450scc. This ternary transient association may catalyze an efficient electron transfer.

Rotational diffusion of P450scc was also very useful for analyzing protein–protein interactions in intact mitochondria (77–79). P450 rotation is measured by observing the time–dependent absorption anisotropy upon photolysis of the heme–CO complex by a vertically polarized laser flash (80–87). In the inner membrane of the mitochondria, the addition of ADX induced mobilization of P450scc by 19% (from 35% to 54%) in the mobile population, but further addition of ADR immobilized

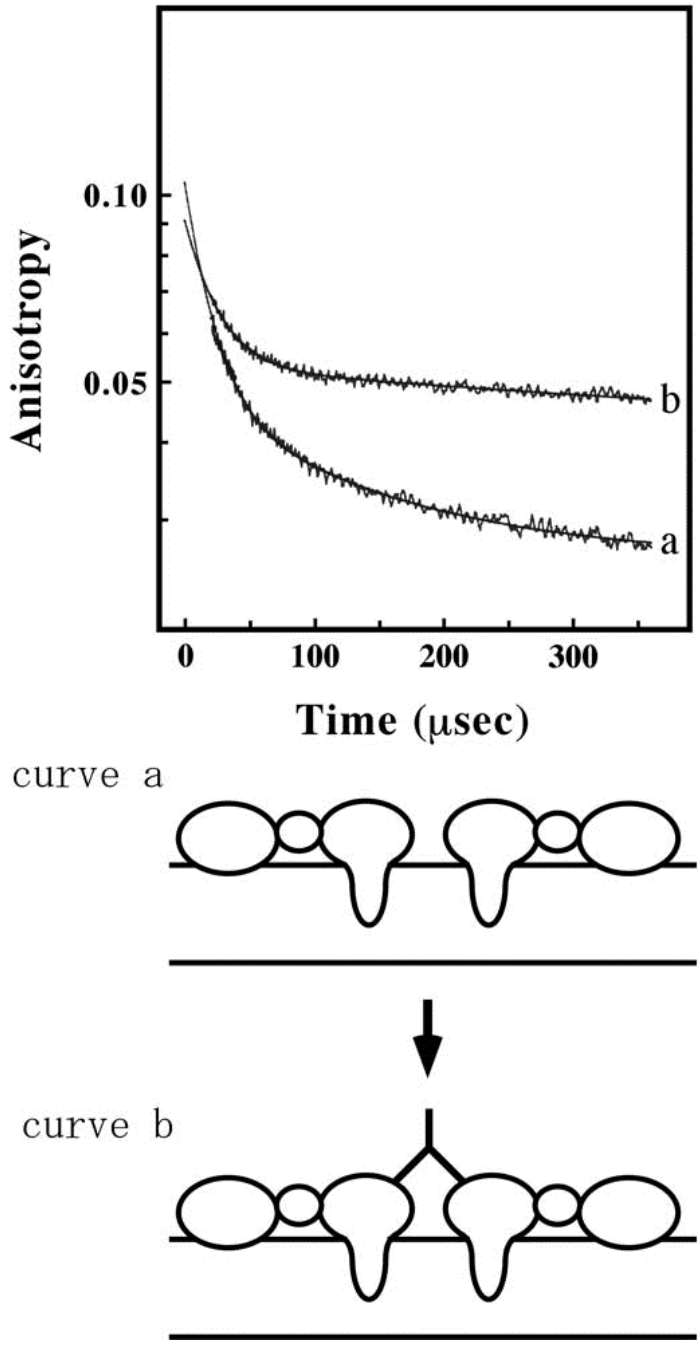

Figure 15

Upper Panel: Phosphorescence anisotropy decay curves of ADR labeled with erythrosin–IA in PC/PE/CL liposomes containing P450scc+ADX+ADR. Curve (a), rotation of ADR in the absence of IgG. Curve (b), Rotation of ADR when anti–P450scc IgG is applied to curve (a). Anti–P450scc IgG significantly suppresses the mobility of ADR, indicating the ternary complex of these proteins. Lower Panel: Schematic model corresponding to curve (a) and curve (b).

P450scc by 6%, implying that a transient ternary complex formed between these three proteins (79).

3.2 Adrenocortical microsomal P450

To investigate whether P450c21 and P45017α, form a transient association with NADPH–cytochrome P450 reductase, purified cytochromes were reconstituted with and without the P450 reductase in PC/PE/phosphatidylserine (PS) vesicles. In the presence of the reductase, 6% of cytochrome P450c21 was mobilized in liposomes, due to dissociation of P450 micro–aggregates, by forming a transient association with reductase (see Fig. 16). Note that the mobility of P45017α, was not significantly affected by reductase. These results indicate that P450c21 forms a transient heterodimeric association with the P450 reductase; P45017α,, however, moves independently of the reductase (87, 88). Electrons may therefore be delivered during the transient association of P450c21 with the reductase. In contrast, electrons may be

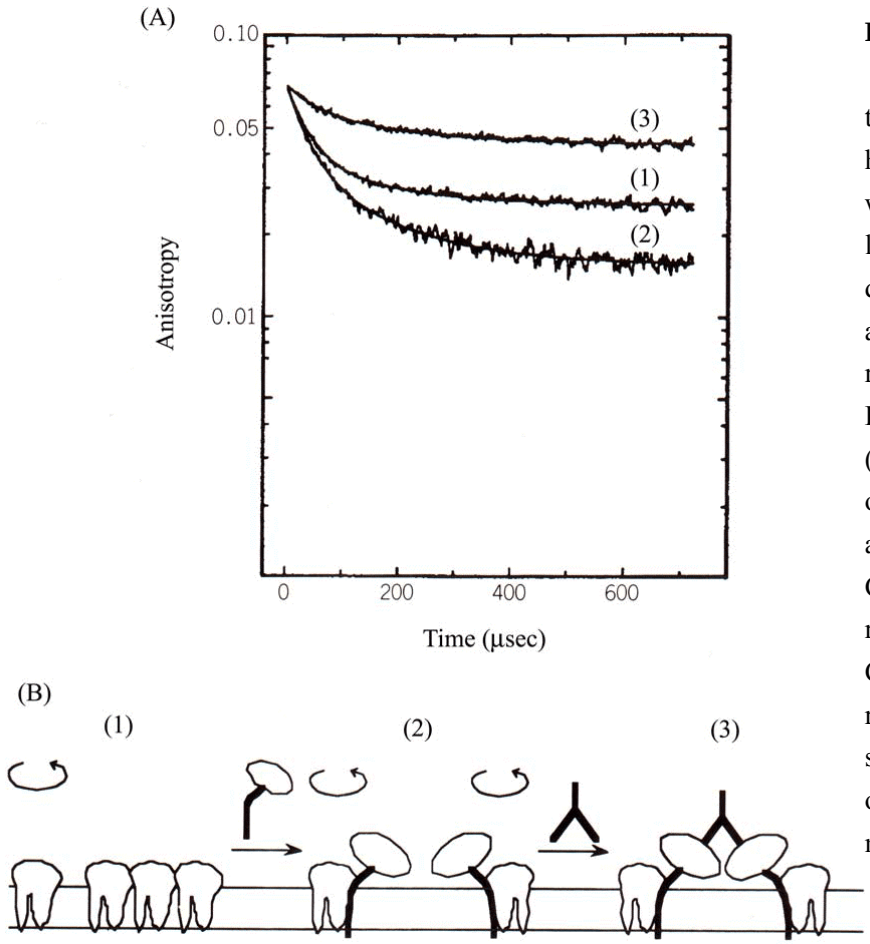

Figure 16

Decay curves demonstrate the formation of transient heterodimeric complex of P450c21 with P450 reductase in PC/PE/PS liposomes. Absorption anisotropy decay curves of P450c21 in Panel (A) and a corresponding model for rotation of P450c21 interacting with P450 reductase in Panel (B). Curve (1), Rotation of P450c21 alone. 90% of P450c21 rotates with ϕ= 200 μsec and the remaining 10% is immobile. Curve (2), The presence of P450 reductase mobilizes P450c21 by 6%. Curve (3), Crosslinking of P450 reductase by the anti–reductase IgG significantly suppresses the mobility of P450c21 down to 40% in the mobile population.

delivered by random collisions between P45017α, and the reductase on the membrane. These results are consistent with kinetic experiments on the rate dependence of the reduction of P450c21, as well as the progesterone hydroxylation activity of P450c21 and P450l7α, on the reductase concentration in liposomes (89). Only a part of P450s in microsomes could form a transient association with the reductase, because the reductase content is very low, at about 1/4–1/10 of the total cytochrome P450 content (90). In contrast with the proteoliposomes, 30–37% of P450 was immobile in microsomes.

3.3 Drug–metabolizing P450 in liver microsomes

Background

There is a huge family of drug–metabolizing P450s in addition to the steroidogenic P450 family. Because there are essential similarities in electron transfer mechanisms between these two different P450 families, we present here several examples. In liver cells, cytochrome P450 catalyzes the oxidative metabolism of various drugs, xenobiotics as well as endogenous substrates (64). Although spectral properties of drug–metabolizing P450s are similar to those of steroidogenic P450s, substrate specificities are markedly different; whereas drug metabolizing P450s may accept a very diverse variety of substrates, the steroidogenic P450s demonstrate strict substrate requirements. Roughly 200 genetically distinct drug–metabolizing P450s have been identified based on cDNA investigations. Their substrate divergence is even wider than their genetic divergence.

The presence of many chemically different species of P450 in liver microsomes prevents the selective analyses of a particular species of P450. In order to perform the rigorous characterization of a specific isoform of P450IA1, we used the heterologous expression of P450IA1 in yeast *Saccaromyces Cerevisiae* microsomes (91–93). These expression systems have also provided a means of examining structure–function relationships through the construction of chimeric proteins. We used fusion proteins between P450IA1

and NADPH–cytochrome P450 reductase in order to examine the effect of complex formation on the mobility of P450 (94). We also used N–terminally truncated P450IA1 in order to examine the membrane topology of P450IA1 (95).

Interactions of Genetically Expressed P450IA1 with P450 Reductase

The methylcholanthrene–inducible cytochrome P450IA1 is known to convert polycyclic aromatic hydrocarbons to highly carcinogenic compounds (96). In a

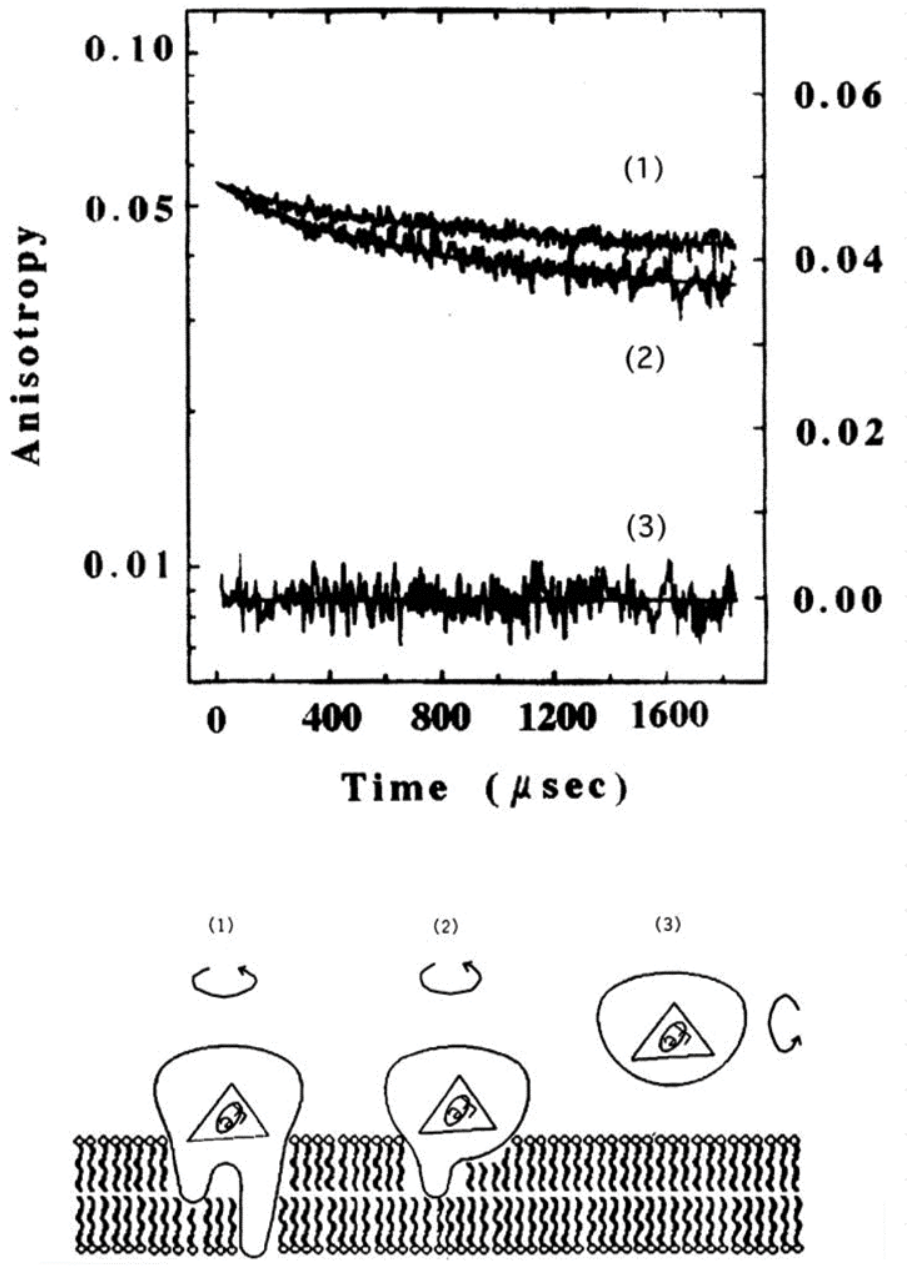

Figure 17

Anisotropy decay curves in Upper Panel and the membrane topology in Lower Panel of liver P450IA1, genetically expressed in yeast microsomes. Curve (1), Rotation of wild type P450IA1. 28% is mobile and the remaining 72% is immobile. Curve (2), Rotation of N–terminary truncated P450IA1△2–30. 41% is mobile (ϕ = 1020 μsec), a result not very different from curve (1). Curve (3), Water soluble bacterial P450cam rotates very rapidly (ϕ <5 μsec), due to being membrane unbound. This results in zero anisotropy on this time scale. Anisotropy of curves (1) and (2) corresponds to the left logarithmic scale, and anisotropy of curve (3) corresponds to the right linear scale.

first experiment, rat liver P450IA1 and/or yeast NADPH–cytochrome P450 reductase was expressed genetically in yeast microsomes. The ratio of P450IA1 to the reductase was about 17:1 and 1:2, without and with coexpression of the reductase, respectively. In microsomes for which only P450IA1 was expressed, 28% of the P450IA1 was rotating. The mobile population was increased to 43% by the presence of the coexpressed reductase **(**see Fig. 17). This significant mobilization of P450IA1 by the presence of reductase implies a transient association of P450IA1 with the reductase (93).

In a second experiment, the fusion protein of rat liver P4501A1 with NADPH–cytochrome P450 reductase was expressed genetically in yeast microsomal membranes. In this case, 40 % of the fusion protein rotated with a rotational relaxation time c of 1351 μsec. The mobile population of the fusion protein is close to that of P4501A1 coexpressed with the P450 reductase, and is greater than that of P4501A1 alone. The large mobile population of the fusion protein between P450IA1 and P450 reductase provides evidence that P4501A1 is mobilized by forming associations with P450 reductase in microsomal membranes (94).

In a third experiment, a modified rat liver cytochrome P450IA1, lacking amino acids 2–30 which is a proposed membrane anchor for P450, was expressed genetically in yeast microsomal membranes. A full–length P450IA1 was also expressed in yeast microsomes. 41% of the shortened P450IA1 was rotating (see Fig.17). A high salt treatment did not remove the shortened cytochrome from the membrane, and also did not drastically weaken the interaction of the cytochrome with the membrane, as judged from the slow rotational characteristics observed (ϕ = 830 μsec). These results demonstrate that the N–terminal–shortened P450IA1 is incorporated properly into the yeast microsomal membrane and that the N–terminal hydrophobic segment is not solely responsible for attachment to the membrane, providing evidence that additional segments of P450IA1 are involved in the membrane binding (95). Our results are consistent with the report that genetically expressed cytochrome P450IIE1 lacking the N–terminal hydrophobic segment tightly binds to the membrane of Escherichia coli (97). Prior to these sophisticated studies using chimeric proteins, microsomal cytochrome P450 was not expected to have deeply membrane–embedded polypeptides, other than the hydrophobic N–terminal segment, as judged from the computer analyses of the amino acid sequences (98, 99).

Dynamic Interactions of P450IIB1, P450IA2 and P450IIB4 with P450 reductase

We investigated the transient interaction between P450 reductase and purified P450IIB1/IA2/IIB4. The three P450s have demonstrated very different interactions with P450 reductase. By the presence of the P450 reductase, the mobile population was increased significantly from 65% to 95% for P450IIB1 (84, 85) and from 80% to 89% for P450IA2 (100), due to the dissociation of P450 oligomers. On the other hand, the mobility of cytochrome P450IIB4 was not considerably affected by the presence of NADPH–cytochrome P450 reductase, a mobile population of 100% being maintained (100). These results imply that cytochromes P450IIB1 and P450IA2 form transient associations with NADPH–cytochrome P450 reductase. Taken together with biochemical experiments, this suggests that cytochrome P450IIB4 diffuses independently of P450 reductase.

We were able to determine the tilt angle of the P450 heme plane from the membrane plane, using the "rotation–about–membrane normal" model, when all cytochrome P450 molecules were completely mobilized in proteoliposomes where the P450 concentration was very low, having a lipid–to–P450 ratio of 10–30 (w/w) (see Methods). Tilt angles were distributed around $55^{\circ} \pm 15^{\circ}$ for all types of P450s as shown in Table 1.

Summary

Neurosteroids are 4th generation neuromessengers. Neurosteroids are promising neuromodulators which either activate or inactivate neuron–neuron communication and thereby mediate learning and memory in the hippocampus. Their synthesis is acutely dependent on Ca^{2+} signals attendant upon neuron–neuron communication, and their actions also acutely modulate neuronal signal transduction via neurotransmitter receptors and membrane steroid receptors

Table 1

The tilt angle of the P450 heme plane from the membrane plane, determined using the "rotation-about-membrane normal" model from the minimal anisotropy of $[r3/r(0)]_{min} = (1/4)(3\cos^2 \theta_N - 1)^2$ (see ref. 79,81,85,87,100,106).

type of P450	tilt angle	$[r_3/r(0)]_{min}$
P45017α,,lyase	47° or 63°	0.04
P450C21	38° or 78°	0.19
P450IIB1/P450IIB2	55°	0.00
P450IA1/P450IA2	48° or 62°	0.03
P450IIB4	55°	0.00
P450scc	55°	
cytochrome oxidase	90°	0.25

(101, 102). As opposed to other neuromessengers such as neurotransmitters, catecholamines and neuropeptides, which are stored in synaptic vesicles and are rapidly exocytosed from presynapses, neurosteroids are produced in mitochondria and microsomes, and are released relatively slowly by passive diffusion in neuronal cells.

Hippocampal neurons are equipped with the complete machinery for the synthesis of PREG(S) and DHEA(S), as well as estradiol and CORT. They are synthesized in mitochondria and microsomes by cytochrome P450s (P450scc, P45017α,, P450arom and P45011β). They then diffuse to fill the interior of the neurons and reach other cells close to steroidogenic neurons because of their amphiphilic characters. The action of steroids based on this spontaneous diffusion is very different from that of neuropeptides, which are secreted from synaptic vesicles. The neurosteroids, PREGS and estradiol, are paracline modulators of neuronal excitability and LTP–induction by rapidly changing an NMDA receptor–mediated Ca^{2+} influx, which in turn induces/reduces the acute synthesis of PREGS and estradiol. The action of estradiol may essentially correlate with the success in estradiol–therapy of Altzheimer's disease of women after menopause. CORT acutely suppresses neuronal excitability by producing an extreme prolongation of the NMDA receptor–mediated Ca^{2+} influx. During stressful situations, the hippocampus itself might synthesize a high concentration of CORT, which acutely suppresses neuron–neuron communication, in addition to peripheral CORT supplied from the adrenal glands. Neurosteroids may, in general, play an essential role in acute modulation of neuronal signal transductions, and in learning and memory, based on emotion such as depression, aggressiveness and protectiveness. The biophysical approach of digital imaging combined with the electrophysiological analysis of neuronal signals, is useful to reveal the mechanisms of signal transductions which accompany the acute action of neurosteroids. Immunohistochemistry, RIA, HPLC analyses are also essential for investigating the synthesis of steroids in the central nervous system.

By comparing the action and synthesis of neurosteroids with that of adrenal/gonadal steroids, we have obtained extended understanding of steroid signal transduction. The structures of essential neurosteroids are the same as those of peripheral steroids; however, their actions are very different with respect to their receptor binding behavior (membrane steroid receptors or nuclear steroid receptors) to the time scales involved in the expression of their effects. Regulation of steroidogenesis in brain neurons seems to be different from that in adrenocortical cells, because neuronal steroidogenesis may occur in postsynaptic neurons (upon pulsed stimulation by neuromessengers) on a time scale of sec to min, whereas steroidogenesis in adrenal glands may be steadily performed, and is slowly regulated by the level of ACTH in the blood, on a time scale of several tens of min. Ca^{2+} signaling plays a role as a second messenger in both the brain and the adrenal cortex. Biochemical characteristics are almost identical for individual steroidogenic proteins between in the brain and peripheral steroidogenic organs. However,

there are great differences between these organs in the amount of steroidogenic proteins, the cholesterol supply and the amount of steroid production.

Rotational diffusion measurements revealed that electron transfer in the P450 systems is performed either by transient complex formation between P450s and P450 reductases or by random collisions between the twos depending on the species of P450. P450s and reductases undergo rapid movement in the membrane, on a time scale of microseconds. These conclusions on electron transfer interactions of P450s may also be valid in central nervous systems, because the DNA sequences of individual steroidogenic proteins are almost identical in the adrenocortical cells and the brain cells.

Acknowledgments

We are very grateful to many graduate students, post docs and visiting professors of Kawato Lab. at the University of Tokyo for the experimental contributions. They are Yasushi Hojo on immunohistochemical study; Yoichiro Ohta and Tomokazu Tsurugizawa and Taka–aki Hattrori on RIA study of neurosteroids; Tomokazu Tsurugizawa, Nobuaki Yasumatsu and Kyoko Hasegawa on electrophysiology study; Jun'ya Makino and Prof. Douglas M. Stocco on StAR study; Norio Takata, Keisuke Shibuya and Dr. Hideo Mukai on NO study; Taiki Takahashi and Taka–aki Hattrori on Ca^{2+} signal study; Ryota Homma, Dr. Yoshihito Niimura and Dr. Alexander Krivosheev on cholesterol–resorufin study; Dr. Tomomitsu Ichikawa and Daisaku Honma, Kazuhiro Suzuki, Hirokazu Sasaki and Tetsuya Urasaki on endosome study, Komatsuzaki for manuscript preparation. Profs. Shiro Kominami and Takeshi Yamazaki at Hiroshima Univ. have essential contribution to neurosteroid metabolism analysis and proteoliposome study. On rotational diffusion study, we are grateful to Prof. Yoshihiro Ohta at Tokyo Univ. of Agriculture and Technology, Dr. Alexander A. Chernogolov from Belarussian Academy, Prof. Galina I. Bachmanova and Prof. Alexander I. Archakov from Russian Medical Academy. We are also grateful to extensive collaborations with Dr. Kazuhiko Yamaguchi at Riken Brain Institute on electrophysiology study, Prof. Richard Cherry and Dr. Ian Morrison at Univ. of Essex on endosome trafficking study, Prof. Takeyuki Hara at Nakamura Gakuen Univ., Prof. Hiro–omi Tamura at Kyoritsu College of Pharmacy, Toshiyuki Sakaki at Kyoto Univ. and Yoshiyasu Yabusaki at Sumitomo Chemical Industry. We thank Dr. John Rose for critical reading of the manuscript. This work is supported by grants from the Ministry of Education, Science and Culture in Japan.

Appendix

Methods for Ca^{2+} signaling measurements and analysis

We used a digital fluorescence microscope which consisted of an inverted microscope (Nikon TMD 300, Japan) equipped with a xenon lamp for excitation and a CCD camera (Hamamatsu Photonics C2400–77 or C–1145, Japan). The glass–bottom dishes were mounted on an inverted microscope equipped with a temperature chamber, which was maintained at 37 deg with high humidity. For fura–2, we changed the excitation wavelength of 340 and 380 nm every 1.15 sec. Fluorescence was measured above 520 nm using a DM510 dichroic mirror and an emission filter. The relative concentrations of Ca^{2+} in individual cells can be estimated from the image analysis of the fluorescence intensity between excitations at 340 nm and 380 nm, with the ARGUS–50 system (Hamamatsu Photonics, Japan). For Calcium Green–1, we selected an excitation wavelength of 450–490 nm and fluorescence above 520 nm with an excitation filter, a dichroic mirror, and an emission filter. For tracing the DiI–LDL in intracellular endosomes, we used a video–enhansed microscope, where data acquision on a video tape and image analysis were performed with ARGUS–50.

Methods for protein rotation measurements

In order to investigate mechanisms of electron transfer between reductases and cytochrome P450s, we have been successfully using protein rotation methods which are very sensitive to protein–protein interactions, over the past 20 years. Protein rotation is revealed to be very sensitive to transient dimer or trimer formation of electron transfer proteins. We initiated this method in 1979, to analyze interactions between P450 and reductase in proteoliposomes (84).

Absorption Anisotropy

Protein rotation of heme proteins may be measured by photolysis of the heme–CO complex by a vertically polarized laser flash, followed by measuring time–dependent depolarization of the absorption anisotropy (78, 81, 103). Cytochrome P450 complexed with CO was photolyzed by a vertically polarized flash at 532 nm from a Nd/YAG laser and the absorbance changes were measured at 450 nm. The signals were analyzed by calculating the absorption anisotropy, r(t), and the total absorbance change, A(t), given by

$$r(t) = [A_V(t) - A_H(t) \cdot S] / A(t) \quad (1)$$

$$A(t) = A_V(t) + 2A_H(t) \cdot S \quad (2)$$

where $A_V(t)$ and $A_H(t)$ are, respectively, the absorption changes for vertical and horizontal polarization at time t after laser flash. In each experiment, 16384 signals were averaged using transient memory.

The analysis of r(t) is based on a model of the axial rotation of cytochrome P450 about the membrane normal (83, 104). When there is a single rotating species of cytochrome P450 with rotational relaxation time $\phi_{\parallel}$, r(t) is given by

$$r(t)/r(0) = 3\sin 2\theta_N \cdot \cos 2\theta_N \cdot \exp(-t/\phi_{\parallel}) + 3/4 \cdot \sin^4\theta_N \cdot \exp(-4t/\phi_{\parallel}) + 1/4(3\cos^2\theta_N - 1)^2 \quad (3)$$

where θ_N is the tilt angle of the heme plane from the membrane plane. Because $\phi_{\parallel}$ is proportional to the square of the membrane–parallel cross–sectional diameter of the protein complex, protein rotation is very sensitive to transient dimer or trimer formation during electron transfer. Multiple rotating species of cytochrome P450 with different $\phi_{\parallel}$ values are considered by analyzing the data using the expressions,

$$r(t) = r1\exp(-t/\phi) + r2\exp(-4t/\phi) + r3 \quad (4)$$

where ϕ is the average rotational relaxation time, taken over multiple rotating species of P450, and r_1, r_2 and r_3 are constants. The population of mobile P450, pm%, was calculated using Eq. 5 on the basis of the experimentally determined minimal anisotropy, $[r_3/r(0)]_{min} = (1/4)(3\cos^2\theta_N - 1)^2$, when all P450 were rotating in proteoliposomes :

$$p_m(\%) = 100x\{1 - r_3/r(0)\}/\{1 - [r_3/r(0)]_{min}\} \quad (5)$$

Phosphorescence Anisotropy

The rotational characteristics of protein labeled with phosphorescent probe may be measured by time–dependent phosphorescence anisotropy decay. The phosphorescent probe erythrosin was excited with a vertically polarized laser flash at 532 nm from a Nd/YAG laser, and the subsequent phosphorescence decay was measured above 640 nm (105). The signal was analyzed by calculating the phosphorescence anisotropy, r(t), and the total phosphorescence intensity $I_T(t)$. Analysis of r(t) for ADR is based on a model of the rapid wobbling of ADR within ADR+ADX+P450 complex which undergoes slow axial rotation in the membrane:

$$r(t) = r_1\exp(-t/\phi_{ADR}) + r_2\exp(-t/\phi_{P450}) \quad (6)$$

where ϕ_{ADR} and ϕ_{P450} are the effective rotational relaxation times of ADR and P450, respectively.

References

1. M. Schumacher, R. Guennoun, P. Robel, and E. E. Baulieu, *Stress*, **2**, 65-78 (1997).
2. C. Corpechot, M. Synguelakis, S. Talha, M. Axelson, J. Sjovall, R. Vihko, E. E. Baulieu, and P. Robel, *Brain Res.*, **270**, 119-125 (1983).
3. P. Robel, E . Bourreau, C. Corpechot, D. C. Dang, F. Halberg, C. Clarke, M. Haug, M. L. Schlegel, M. Synguelakis, C. Vourch, E.-E. Baulieu *J. Steroid Biochem.* 27, 649-655 (1987)
4. S. M. Paul, and R. H. Purdy, *FASEB J.*, **6**, 2311-2321 (1992).
5. G. Dayanithi, and L. Tapia-Arancibia, *J. Neurosci.*, **16,** 130-136 (1996).
6. E. E. Baulieu, *Recent progress in hormone research*, **52**, 1-32 (1997).
7. R. P. Irwin, N. J. Maragakis, M. A. Rogawski, R. H. Purdy, D. H. Farb, and S. M. Paul, *Neurosci. Lett.*, **141**, 30-34 (1992).
8. J. M. Fahey, D. G. Lindquist, G. A. Pritchard, and L. G. Miller, *Brain Res.*, **669**, 183-188 (1995).
9. F. S. Wu, T. T. Gibbs, and D. H. Farb, *Mol. Pharmacol.*, **40**, 333-336 (1991).
10. M. R. Bowlby, *Mol. Pharmacol*., **43**, 813-819 (1993).
11. R. P. Irwin, S. Z. Lin, M. A. Rogawski, R. H. Purdy, and S. M. Paul, *J. Pharmacol. Exp. Ther.*, **271**, 677-682 (1994).
12. T. J. Teyler, R. M. Vardaris, D. Lwis, and A. B. Rawitch, *Science*, **209**, 1017-1019 (1980).
13. M. R. Foy, J. Xu, X. Xie, R. D. Brinton, R. F. Thompson, and T. W. Berger, *J. Neurophisiol.*, **81**, 925-929 (1999).
14. K. Ito, K. L. Skinkle, and T. P. Hicks, *J. Physiol.*, **515**, 209-220 (2000).
15. J. F. Flood, J. E. Morley, and E. Roberts, *Proc. Natl. Acad. Sci. USA*, **89**, 1567-71 (1992).
16. J. F. Flood, J. E. Morley, and E. Roberts, *Proc. Natl. Acad. Sci. USA*, **92**, 10806-10810 (1995).
17. M. Vallee, W. Mayo, M. Darnaudery, C. Corpechot, J. Young, M. Koehl, M. Le Moal, E. E. Baulieu, P. Robel, and H. Simon, *Proc. Natl. Acad. Sci. USA*, **94**, 14865-14870 (1997).
18. S. H. Mellon, and C. F. Deschepper, *Brain Res.*, **629**, 283-292 (1993).
19. J. L. Sanne, and K. E. Krueger, *J. Neurochem.*, **65**, 528-536 (1995).
20. G. Pelletier, V. Luu-The, and F. Labrie, *Brain Res.*, **704**, 233-239 (1995).
21. S. Beyenburg, M. Watzka, I. Blumcke, J. Schramm, F. Bidlingmaier, C. E. Elger, and B. Stoffel-Wagner, *Epilepsy Research*., **41**, 83-91 (2000).
22. C. E. Gomez-Sanchez, M. Y. Zhou, E. N. Cozza, H. Morita, M. F. Foecking, E. P. Gomez-Sanchez, *Endocrinology*, **138**, 3369-73, (1997).
23. S. Kawato, T. Kimoto, Y. Ohta, T. Tsurugizawa, J. Makino, Y. Hojo, and T. Takahashi, in *Molecular Steroidogenesis* (M. Okamoto, Y. Ishimura, and H. Nawata, Eds.) pp385-388, Universal Academy Press, Tokyo (1999)
24. T. Kimoto, T. Tsurugizawa, Y. Ohta, J. Makino, H., Tamura, Y. Hojo, N. Takata, and S. Kawato, *Endocrinology*, **142**, 3578-3589 (2001).
25. S. M. Hsu, L. Raine, and H. J. Fanger, *Hiostochem. Cytochem.*, **29**, 577-58 (1981).
26. R. Guennoun, R. J. Fiddes, M. Gouezou, M. Lombes, and E. E. Baulieu, *Mol. Brain Res.*, **30**, 287-300 (1995).
27. A. Furukawa, A. Miyatake, T. Ohnishi, and Y. Ichikawa, *J. Neurochem.*, **71**, 2231-2238 (1998).
28. C. Le Goascogne, P. Robel, M. Gouezou, N. Sananes, E. E. Baulieu, and M. Waterman, *Science*, **237**, 1212-1215 (1987).
29. K. Iwahashi, H. S. Ozaki, M. Tsubaki, J. Ohnishi, Y. Takeuchi, and Y. Ichikawa, *Biochim. Biophys. Acta*, **1035**, 182-189 (1990).
30. I. Jung-Testas, Z. Y. Hu, E. E. Baulieu, and P. Robel, *Endocrinology*, **125**, 2083-2091 (1989).
31. T. Kimoto, H. Asou, Y. Ohta, H. Mukai, A. A. Chernogolov, and S. Kawato, *J. Pharm. Biomed. Anal.*, **15**, 1231-1240 (1997).
32. T. Takahashi, T. Kimoto, and S. Kawato, in *Molecular Steroidogenesis* (M. Okamoto, Y. Ishimura, and H. Nawata, Eds.) pp407-408, Universal Academy Press, Tokyo (1999).
33. M. Wong, and R. L. Moss, *J. Neuroendocrinol.*, **6**, 347-55 (1994).
34. H. Kojima, Y. Urano, K. Kikuchi, T. Higuchi, Y. Hirata, and T. Nagano, *Angew. Chem. Int. Ed.*, 38, 3209-3212 (1999).
35. N. Takata, T. Kimoto, T. Takahashi, H. Kojima, S. Kominami, T. Nagano, and S. Kawato, in *Molecular Steroidogenesis* (M. Okamoto, Y. Ishimura, and H. Nawata, Eds.) pp409, Universal Academy Press, Tokyo (1999).
36. S. Uchino, Y. Kudo, W. Watanabe, S. Nakajima-Iijima, and M. Mishina, *Molec. Brain. Res.*, **44**, 1-11 (1997).
37. H. Mukai, S. Uchino, and S. Kawato, *Neurosci. Lett.*, **282**, 93-96 (2000).
38. M. Rey, E. Carlier, M. Talmi, and B. Soumireu-Mourat, *Neuroendocrinol.*, **60**, 36-41 (1994).
39. B. S. McEwen, *Cell. Mol. Neurobiol.*, **16**, 103-116 (1996).
40. C. Pavlides, S. Ogawa, A. Kimura, and B. S. McEwen, *Brain Res.*, **738**, 229-35 (1996).
41. L. P. Reagan, and B. S. McEwen, *J. Chem. Neuroanat.*, **13**, 149-167 (1997).
42. S. M. Nair, T. R. Werkman, J. Craig, R. Finnell, M. Joels, and J. H. Eberwine, *J. Neurosci.*, **18**, 2685-2696 (1998).
43. M. P. Armanini, C. Hutshins, B. A. Stein, and R. M. Sapolsky, *Brain Res*., **532,** 7-12 (1990).
44. C. S. Woolley, E. Gould, and B. S. McEwen, *Brain Res.*, **531**, 225-231 (1990).
45. Y. Watanabe, E. Gould, and B. S. McEwen, *Brain Res.*, **588**, 341-345 (1992).
46. M. Joels, *Frontiers in Neuroendocrinology*, **18**, 2-48 (1997).
47. M. -X. Tang, D. Jacobs, Y. Stern, K. Marder, P. Schofield, B. Gurland, H. Andrews, and R. Mayeux, *Lancet*, **348**, 429-432 (1996).
48. P. Collins, and C. Webb, *Nature Med.*, **5**, 1130-1 (1999).
49. R. Bi, G. Broutman, M. R. Foy, R. F. Thompson, and M. Baudry, *PNAS*, **97**, 3602-3607 (2000).
50. J. Z. Tsien, D. F. Chen, D. Gerber, C. Tom, E. H. Mercer,

D. J. Anderson, M. Mayford, E. R. Kandel and S. Tonegawa, *Cell*, 87, 1317-1326 (1996).
51. J. Z. Tsien, P. T. Huerta, and S. Tonegawa, *Cell*, **87**, 1327-1338 (1996).
52. K. Ukena, M. Usui, C. Kohchi, and K. Tsutsui, *Endocrinology*, **139**, 137-147 (1998).
53. K. Tsutsui, K. Ukena, M. Usui, H. Sakamoto, and M. Takase, *Neuroscience Research* 36, 261-273 (2000)
54. M. Stromstedt, and M. R. Waterman, *Mol. Brain Res*., **34**, 75-88 (1995).
55. P. Guarneri, D. Russo, C. Cascio, G. De Leo, F. Piccoli, and R. Guarneri, *Eur. J. Neurosci*., **10**, 1752-1763 (1998).
56. P. Guarneri, R. Guarneri, C. Cascio, P. Pavasant, F. Piccoli, and V. Papadopoulos, *J. Neurochem*., **63**, 86-96 (1994).
57. M. D. Majewska, S. Demirgoren, and E. D. London, *Eur. J. Pharmacol*., **189**, 307-15 (1990).
58. S. Demirgoren, M. D. Majewska, C. E. Spivak, and E. D. London, *Neurosci*., **45**, 127-35 (1991).
59. F. Le Foll, E. Louiset, H. Castel, H. Vaudry, and L. Cazin, *Eur. J. Pharmacol*., **331**, 303-311 (1997).
60. T. Hattori (Kawato Lab.) in *Master thesis*, Univ. of Tokyo (2001)
61. C. Beyer, and H. Raab, *Eur. J. Neurochem*., 10, 255-262 (1998)
62. B. S. McEwen, and R. M. Sapolsky, *Curr. Opin. Neurobiol*., **5**, 205-216 (1995).
63. A. Rami, A. Rabie, and J. Winckler, *Exp. Neurol*., **149**, 439-446 (1998).
64. T. Omura, Y. Ishimura, and Y. Fujii-Kuriyama, (eds.) *Cytochrome P450*, second edition, VCH publishers, Kodansha (1993).
65. T. Kimura, *Mol. Cell. Biochem*., **36**, 105-122 (1981).
66. B. Cheng, D. K. Hsu, and T. Kimura, *Molec. Cell. Endocrinol*., **40**, 233-243 (1985).
67. D. G. Grahame-Smith, R. W. Butcher, R. L. Ney, and E. W. Sutherland, *J. Biol. Chem*., **242**, 5535-5541 (1967).
68. K. Yanagibashi, V. Papadopoulos, E. Masaki, T. Iwaki, M. Kawamura, and P. F. Hall, *Endocrinology*, **124**, 2383-2391 (1989).
69. T. Kimoto, Y. Ohta, and S. Kawato, *Biochem. Biophys. Res. Commun*., **221**, 25-30 (1996).
70. T. Kimoto, Y. Ohta, and S. Kawato, *Bioimages*, **5**, 133-142 (1997).
71. T. Yamazaki, T. Kimoto, K. Higuchi, Y. Ohta, S. Kawato, and S. Kominami, *Endocrinology*, **139**, 4765-71 (1998).
72. R. Homma, T. Kimoto, Y. Niimura, A. Krivosheev, T. Hara, Y. Ohta, and S. Kawato, *J. Inorg. Chem*., **82**, 171-180 (2000).
73. Y. Brandenburger, E. D. Kennedy, C. P. Python, M. F. Rossier, M. B. Vallotton, C. B. Wollheim, and A. M. Capponi, *Endocrinology*, **137**, 5544-51 (1996).
74. T. Rohacs, K. Tory, A. Dobos, and A. Spat, *Biochem. J*., **328**, 525-8 (1997).
75. T. Rohacs, G. Nagy, and A. Spat, *Biochem. J*., **322**, 785-92 (1997).
76. T. Ichikawa, M. Yamada, D. Honma, R. J. Cherry, I. E. G. Morrison, and S. Kawato, *Biochem. Biophys. Res. Commun*., **269**, 25-30 (2000).
77. S. Kawato, F. Mitani, T. Iizuka, and Y. Ishimura, *J. Biochem*., **104**, 188-91 (1988).
78. Y. Ohta, F. Mitani, Y. Ishimura, K. Yanagibashi, M. Kawamura, and S. Kawato, *J. Biochem*., **107**, 97-104, (1990).
79. Y. Ohta, K. Yanagibashi, T. Hara, M. Kawamura, and S. Kawato, *J. Biochem*., **109**, 594-9 (1991).
80. S. Kawato, E. Sigel, E. Carafoli, and R. J. Cherry, *J. Biol. Chem*., **255**, 5508-10 (1980).
81. S. Kawato, E. Sigel, E. Carafoli, and R. J. Cherry, *J. Biol. Chem*., **256**, 7518-7527 (1981).
82. S. Kawato, C. Lehner, M. Muller, and R. J. Cherry, *J. Biol. Chem*., **257**, 6470-6 (1982).
83. S. Kawato, J. Gut, R. J. Cherry, K. H. Winterhalter, and C. Richter, *J. Biol. Chem*., **257**, 7023-9 (1982).
84. J. Gut, C. Richter, R. J. Cherry, K. H. Winterhalter, and S. Kawato, *J. Biol. Chem*., **257**, 7030-6 (1982).
85. J. Gut, C. Richter, R. J. Cherry, K. H. Winterhalter, and S. Kawato, *J. Biol. Chem*., **258**, 8588-94 (1983).
86. J. Gut, S. Kawato, R. J. Cherry, K. H. Winterhalter, and C. Richter, *Biochimica et Biophysica Acta*, **817**, 217-28 (1985).
87. Y. Ohta, S. Kawato, H. Tagashira, S. Takemori, and S. Kominami, *Biochemistry*, **31**, 12680-7 (1992).
88. S. Kominami, H. Tagashira, Y. Ohta, M. Yamada, S. Kawato, and S. Takemori, *Biochemistry*, **32**, 12935-12940 (1993).
89. S. Kominami, S. Inoue, A. Higuchi, and S. Takemori, *Biochimica et Biophysica Acta*, **985**, 293-9 (1989).
90. S. Takemori, and S. Kominami, in *Molecular Mechanisms of Adrenal Steroidogenesis and Aspects of Regulation and Application* (K. Ruckpaul, and H. Rein, Eds.) pp153-203, Akademie-Verlag, Berlin (1990).
91. T. Sakaki, M. Shibata, Y. Yabusaki, and H. Ohkawa, *DNA*, **6**, 31-9 (1987).
92. H. Murakami, Y. Yabusaki, T. Sakaki, M. Shibata, and H. Ohkawa, *J. Biochem*., **108**, 859-65 (1990).
93. T. Iwase, T. Sakaki, Y. Yabusaki, H. Ohkawa, Y. Ohta, and S. Kawato, *Biochemistry*, **30**, 8347-51 (1991).
94. M. Yamada, Y. Ohta, T. Sakaki, Y. Yabusaki, H. Ohkawa, and S. Kawato, *Biochemistry*, **38**, 9465-70 (1999).
95. Y. Ohta, T. Sakaki, Y. Yabusaki, H. Ohkawa, and S. Kawato, *J. Biol. Chem*., **269**, 15597-600 (1994).
96. F. P. Guengerich, (ed) *Mammalian Cytochrome P-450*, Vol. 2, CRC Press, Boca Raton, FL (1987).
97. J. R. Larson, M. J. Coon, and T. D. Porter, *J. Biol. Chem*., **266**, 7321-4 (1991).
98. D. R. Nelson, and H. W. Strobel, *J. Biol. Chem*., **263**, 6038-6050 (1988).
99. O. Gotoh, and Y. Fujii-Kuriyama, in *Frontiers in Biotransformation* (K. Ruckpaul, and H. Rein, Eds.) Vol. 1 pp. 195-243, Akademie-Verlag, Berlin (1989).
100. M. Yamada, Y. Ohta, G. I. Bachmanova, Y. Nishimoto, A. I. Archakov, and S. Kawato, *Biochemistry*, **34**, 10113-9 (1995).
101. F. B. Moore, and S. Evans, *Brain Behav. Evol*., **54**, 41-50 (1999)
102. E. Falkenstein, H. –C. Tillmann, M. Christ, M. Feuring, and M. Wehling., *Pharmacol. Rev*., **52**, 513-555 (2000)
103. R. J. Cherry, *Methods Enzymol*., **54**, 47-61 (1978)
104. S. Kawato, and K. Kinosita, Jr. *Biophys. J*., **36**, 277-96 (1981).
105. K. Kinosita, Jr., S. Ishiwata, H. Yoshimura, H. Asai, A.

Ikegami, *Biochemistry*, 23, 5963-5975 (1984).
106. H. U. Etter, C. Richter, Y. Ohta, K. H. Winterhalter, H. Sasabe, S. Kawato, *J. Biol. Chem.*, 266, 18600-5 (1991).